

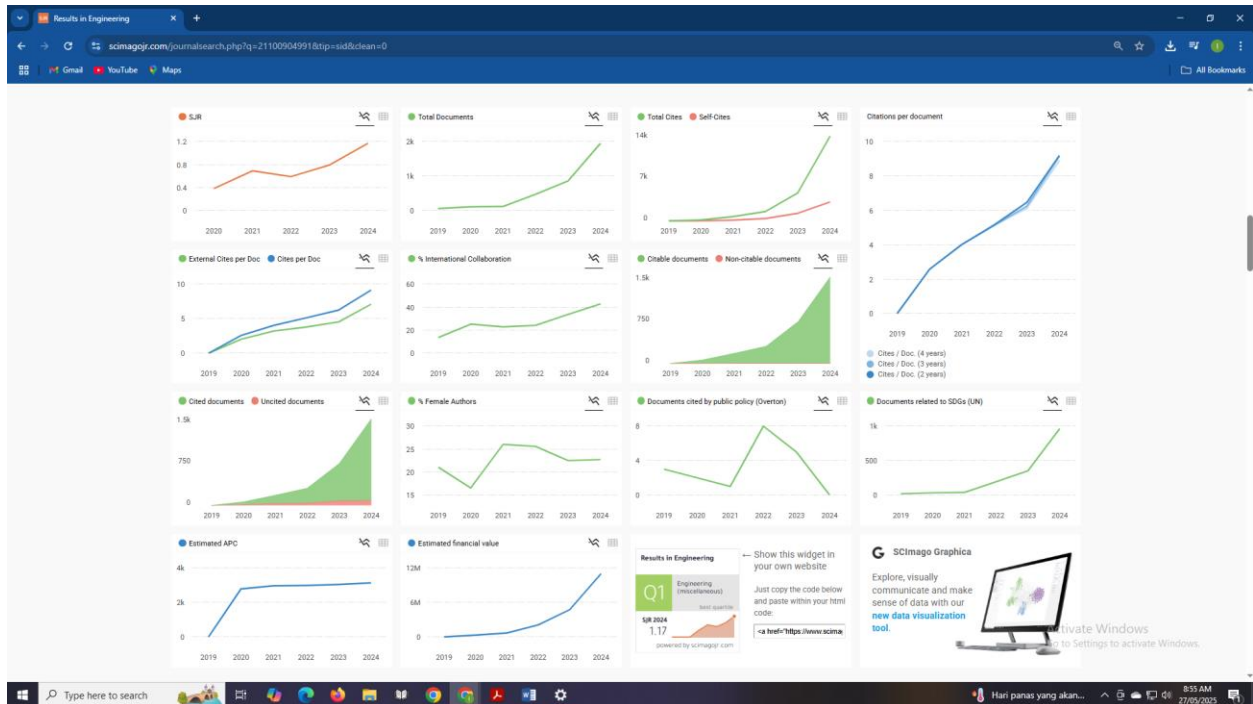
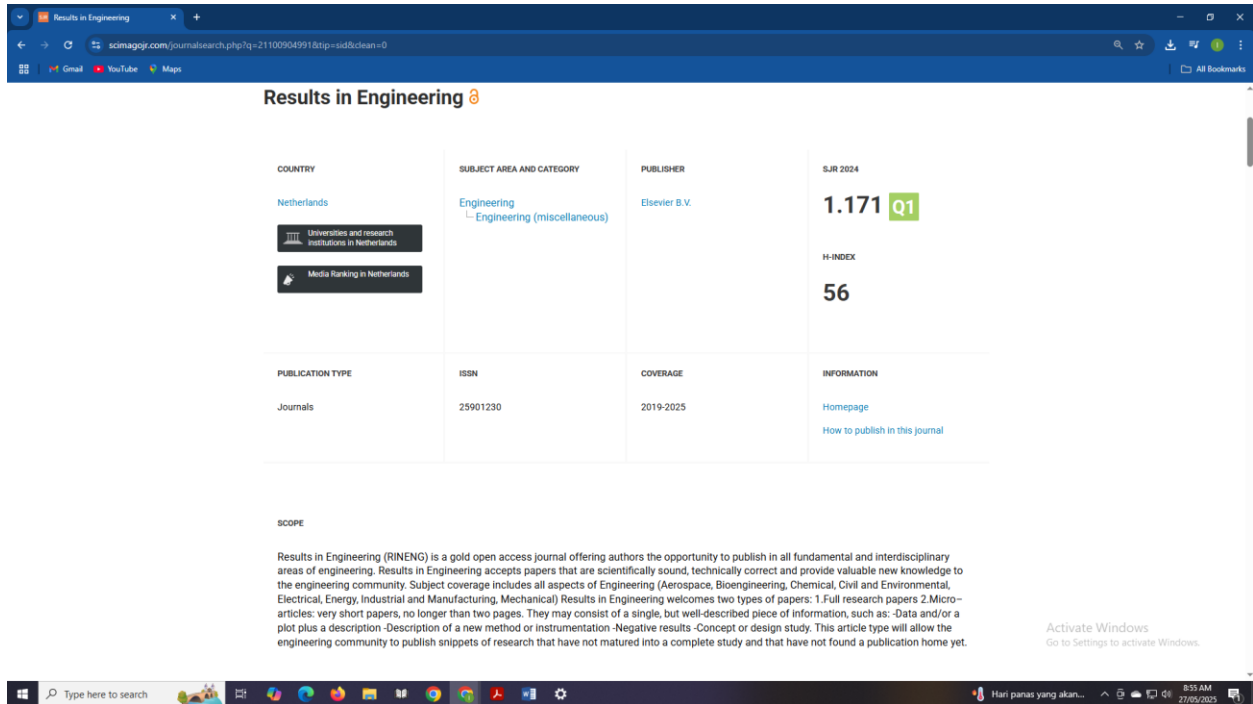
Deskripsi Artikel

- Judul Jurnal : Result in Engineering
- Volume Jurnal : Vol. 16, December 2022.
- Judul Artikel : Perforated Concave Rectangular Winglet Pair Vortex Generators Enhance The Heat Transfer Of Air Flowing Through Heated Tubes Inside A Channel.
- Penulis : **Oktarina Heriyani**, Mohammad Djaeni, Syaiful , Aldila Kurnia Putri.
- Status Penulis : Kontributor
- Peringkat : Q1

Results in Engineering

Properties Q1

<https://www.scimagojr.com/journalsearch.php?q=21100198926&tip=sid&clean=0>



Link Jurnal

<https://www.sciencedirect.com/journal/results-in-engineering>

The screenshot shows the homepage of the 'Results in Engineering' journal. The header includes the ScienceDirect logo and navigation links like 'Journals & Books', 'Help', 'Search', 'My account', and 'Sign in'. The main banner features the journal's title, 'Open access' status, and its metrics: CiteScore 5.8 and Impact Factor 6.0. Below the banner, there are links for 'Articles & Issues', 'About', 'Publish', and a search bar. The 'About the journal' section describes it as a gold open access journal. The 'Article publishing option' section details the Open Access policy and APC. A timeline shows key milestones: 12 days to first decision, 61 days review time, 74 days submission to acceptance, and 8 days acceptance to publication. The footer lists the Executive Editors and a link to the Editorial Board.

Results in Engineering
Open access

CiteScore 5.8 | Impact Factor 6.0

[Articles & Issues](#) [About](#) [Publish](#) [Search in this journal](#) [Submit your article](#) [Guide for authors](#)

About the journal
Results in Engineering (RINENG) is a **gold open access** journal offering authors the opportunity to publish in all fundamental and interdisciplinary areas of engineering. Results in Engineering accepts papers that are **scientifically sound, technically correct and provide valuable new knowledge** to the ...
[View full aims & scope](#)

Article publishing option
Open Access
Article Publishing Charge (APC): **USD 1,810 (excluding taxes)**. This journal is taking part in the GPOA pilot. [Review this journal's open access policy.](#)

12 days Time to first decision
61 days Review time
74 days Submission to acceptance
8 days Acceptance to publication
[View all insights](#)

Executive Editors - Biomedical Engineering and Bioengineering Applications

Link Editorial Board

<https://www.sciencedirect.com/journal/results-in-engineering/about/editorial-board>

The screenshot shows the Editorial Board page for 'Results in Engineering'. It features a header with the journal's title and metrics. The main content is divided into two sections: 'Editorial board' and 'Executive Editors'. The 'Editorial board' section includes a pie chart showing the gender diversity of editors and board members: 88% men, 13% women, 1% non-binary or gender diverse, and 1% prefer not to disclose. The 'Executive Editors' section lists two editors: Professor Stavros Kassinos (Biomedical Engineering and Bioengineering Applications) and Professor Suresh C. Pillai (Chemical & Environmental). The footer lists the Civil, Structural and Materials section.

Results in Engineering
Open access

CiteScore 5.8 | Impact Factor 6.0

[Articles & Issues](#) [About](#) [Publish](#) [Search in this journal](#) [Submit your article](#) [Guide for authors](#)

Editorial board

Gender diversity of editors and editorial board members

88% men
13% woman
1% non-binary or gender diverse
1% prefer not to disclose

Executive Editors
Biomedical Engineering and Bioengineering Applications

Professor Stavros Kassinos
University of Cyprus Department of Mechanical & Manufacturing Engineering, Lefkosia, Cyprus
computational fluid dynamics, respiratory biomechanics and physiology, drug delivery, turbulence simulation and modeling, machine learning and in-silico population studies
[View full biography](#)

Chemical & Environmental

Professor Suresh C. Pillai
Atlantic Technological University - Sligo, Sligo, Ireland
Nanotechnology, Energy Materials, Supercapacitors, Photocatalysis, Electronic Materials, Advanced Functional Materials, Engineering Materials and Ceramics
[View full biography](#)

Civil, Structural and Materials

Link Daftar isi

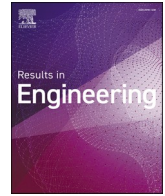
<https://www.sciencedirect.com/journal/results-in-engineering/vol/16/suppl/C?page=2>

The screenshot shows the journal page for Results in Engineering, Volume 16, December 2022. The page features a navigation bar at the top with links to Articles & Issues, About, Publish, and Search. Below the navigation bar, there are buttons for 'Previous vol/issue' and 'Next vol/issue'. The main content area is divided into two columns. The left column contains a sidebar with 'Actions for selected articles' (Download PDFs, Export citations, Show all article previews) and a 'Contents' list (Reviews, Regular papers, Short communication, Micro-article, Special issue on Multi-Material Printed Electronic Components and Devices, Special issue on RINENG Young Investigator Award-2022). The right column displays a list of articles, including 'Perforated concave rectangular winglet pair vortex generators enhance the heat transfer of air flowing through heated tubes inside a channel' by Oktarina Heriyani, Mohammad Djoeni, Syaiful, and Aldila Kurnia Putri. The page also includes a 'Sign in to set up alerts' button and a 'FEEDBACK' button.

Link Artikel

<https://www.sciencedirect.com/science/article/pii/S2590123022003759>

The screenshot shows the article page for 'Perforated concave rectangular winglet pair vortex generators enhance the heat transfer of air flowing through heated tubes inside a channel' by Oktarina Heriyani, Mohammad Djoeni, Syaiful, and Aldila Kurnia Putri. The page features a navigation bar at the top with links to Journals & Books, Help, Search, My account, and Sign in. Below the navigation bar, there are buttons for 'View PDF' and 'Download full issue'. The main content area is divided into three columns. The left column contains a sidebar with 'Outline' (Highlights, Abstract, Keywords, Introduction, Experimental approach, Results and discussion, Conclusion, Credit author statement, Declaration of competing interest, Acknowledgements, References, Show full outline) and 'Cited by (14)'. The middle column displays the article title, authors, and a 'Highlights' section. The right column contains 'Recommended articles' and 'Article Metrics' (Citations, Citation Indexes, Captures, Mendeley Readers, Mentions, News Mentions). The page also includes a 'FEEDBACK' button.



Perforated concave rectangular winglet pair vortex generators enhance the heat transfer of air flowing through heated tubes inside a channel

Oktarina Heriyani^{a,b,*}, Mohammad Djaeni^a, Syaiful^{a,**}, Aldila Kurnia Putri^a

^a Mechanical Engineering Department, Engineering Faculty, University of Diponegoro, Semarang, Indonesia

^b Mechanical Engineering Program, Engineering Faculty, University of Muhammadiyah Prof. DR. HAMKA, Jakarta, Indonesia

ARTICLE INFO

Keywords:

Perforated
Rectangular winglet
Concave
Pressure drop
Vortex generator
Heat transfer
Thermal performance

ABSTRACT

A significant increase in the rate heat transfer in a heat exchanger system is made possible by increasing the convection heat-transfer coefficient using a passive method. The addition of vortex generators (VGs) to the fins and tubes of a heat exchanger is currently the most effective passive method. However, the increase in heat was accompanied by an increase in pressure drop. Therefore, in this study, we installed perforated concave rectangular winglet pair vortex generators (PCRWP VGs) on plates in rectangular ducts to increase the heat transfer through the six heated tubes to the air stream by lowering the enhancement in the pressure drop. We attempted to determine the best cost-benefit ratio (*CBR*) with a fluid flow velocity difference of 0.4–2 m/s at intervals of 0.2 m/s (Reynolds number (*Re*) of 2143 to 11,763) in the channel. The PCRWP VGs were composed of in-line and staggered configurations. The results showed a lower *CBR* (3.56) for the in-line configuration than for the staggered configuration. Moreover, the lowest *CBR* was accompanied by an increase in thermal performance (*TEF*) of 1.29.

1. Introduction

The global energy demand is expected to triple over the next few years. According to a statement by the International Energy Agency (IEA), the main driver is the increasing use of air conditioning (AC) machines [1]. Thus, promoting energy efficiency in air conditioners is important and requires maximising their thermal performance, which involves increasing the rate of heat transfer in its main component, i.e., the condenser. A condenser, commonly used in air conditioners, comprises a fin and a tube and functions as a refrigerant cooling medium. However, the high thermal resistance (75%) of the fin air side of the condenser lowers the heat-transfer rate in the heat exchanger [2]. Thus, the thermal resistance must be lowered to enhance the heat transfer rate.

A commonly used active methods to increase the rate of heat transfer involves adding vortex generators (VGs), which, according to the research results obtained by Mugisidi et al., increases the performance of a condenser [3]. The added VGs cause longitudinal vortices (LVs), damage the primary flow, make the second flow as large as the first and increase air mixing in the area [4,5]. The size of the LVs, shape of the flow, and mixing are influenced by the shape, geometry and position of

the VGs added to the fins and tubes of the heat exchanger [6].

Samidifat et al. showed that simple rectangular vortex generators (RVGs) can increase the heat transfer rate by 7%; however, this causes a pressure drop in the heat exchanger system [7]. Meanwhile, modified RVGs with a concave shape on the front and rear surfaces decreased the heat transfer performance of the heat exchanger tube. A better option is to use RVGs with a double convex front surface and a single concave back surface, which can strengthen the primary vortex, increasing the rate of heat transfer from the plate to the fluid, as demonstrated in a study by Kashyap et al. [8]. Further research conducted by Kashyap et al. in the same year concluded that modifying the surface shape of rectangular winglet vortex generators (RWVGs) can create longitudinal eddies that interact with the boundary layer, thereby increasing the rate of convection heat transfer [9]. Based on their research, the increase in the optimal heat transfer rate was 14.4. The optimal heat transfer performance was also obtained from the results of experiments conducted by Adnan et al. on rectangular ducts by adding delta and rectangular winglet VGs [10]. Concave curved delta winglet VGs were compared with convex curved delta winglet VGs by Song et al. to observe changes in the heat transfer rate [11]. The results showed that the concave VGs

* Corresponding author. Mechanical Engineering Department, Engineering Faculty, University of Diponegoro, Semarang, Indonesia.

** Corresponding author.

E-mail addresses: oktarina@uhamka.ac.id (O. Heriyani), syaiful.undip2011@gmail.com (Syaiful).

improved the heat transfer better than the convex VGs. The differences in the shape of the VGs affects the change in the heat transfer rate and the change in the geometry of the VG, such as a new rib geometry in the cylinder channel [12].

Zeeshan et al. showed that increasing the angle of attack increased the rate of heat transfer (to 37.01–64.54%) if a pair of RWVGs were placed at the back of the tube even though this did not reduce the pressure drop [13]. A decrease in the value of the pressure drop also did not occur significantly, even though there was an increase in heat of 260% in heat, as per the results of the research conducted by Linardo et al. using the batched heat and channelled pipe (BHCP) approach [14]. The increase in heat transfer performance is influenced by the number of RWVG pairs based on the research results of Heriyani et al., where there is an increase in the hydraulic thermal performance evaluation criteria by 15.17% for three pairs of RWVG compared with the baseline [15]. Wang et al. found that the more pairs of VGs placed in the crossflow, the higher the increase in the heat transfer coefficient [16]. Sun et al. further discovered that increasing the number of RWVGs in the heat exchanger tube increased the heat transfer, with a maximum thermal enhancement factor (*TEF*) of 1.27 [17]. The *TEF* value of a V-delta winglet VG reached 1.82–3% higher than that of a V-rectangular winglet VG, as revealed by Promvong et al. [18]. These results were obtained with an optimal blockage ratio (*BR*) of 0.15 and pitch ratio (*PR*) 1.0. Skullong et al. modified the shapes of RWVGs with optimal *BR*s and *PR*s to achieve an optimum heat transfer performance and reduced pressure drop; their shape modification involved perforating RWVGs [19].

The positions of the holes in the RWVGs did not significantly affect the increase in heat transfer; however, they significantly affected the flow resistance of the VGs. The heat-transfer rate increased as the height (vertical position) of the hole increased. Widthwise, although there is an initial increase, the heat transfer rate decreased with increasing lateral distance [20]. An increase in the number of holes in the RWVGs indicates an increase in fluid flow, which forces the fluid to flow behind the RWVGs, thereby increasing heat transfer [4]. The heat transfer rate increased during laminar flow when the Reynolds number (*Re*) increased and then decreased with an increase in *Re* during turbulent flow [20]. Positioning the tube in-line with a pair of RWVGs in a common flow-down configuration provides better performance than the common flow-up configuration. However, a staggered tube position is

superior, resulting in a 25.85% higher heat-transfer performance than when a pair of RWVGs is not used [21].

In the existing studies, no detailed analyses of heat transfer were conducted on from the surfaces of several cylinders heated and arranged in-line when using a perforated vortex generator. Therefore, the focus herein is on investigating the advantages of using perforated concave rectangular winglet pair vortex generators (PCRWP VGs) to increase the heat transfer of the airflow through heated tubes arranged in-line in the ducts.

2. Experimental approach

2.1. Experimental setup

This research was conducted experimentally with a test equipment scheme comprising a rectangular channel sized $370 \times 18 \times 8$ cm. The duct was made of 1 cm thick glass, as shown in Fig. 1.

Based on Fig. 1, the rectangular channel is equipped with a blower (50 Hz, Wipro with a rated voltage of 220 V), an inverter (Mitsubishi Electric type FR-D700 with an accuracy of 0.01), straightener, hot wire anemometer (Lutron type AM-4204 with an accuracy of 0.1), wattmeter (Lutron DW-6060 with an accuracy ± 1.0), central processing unit (CPU), micromanometer, thermocouple (K type with a temperature interval of -200 – 1250 °C and an accuracy ± 0.5) where one thermocouple was placed in the air inlet area, six thermocouples on the back surface of the tubes and 15 on the outlet side of the wire, data acquisition (Advantech USB-4718 type with an accuracy of 0.001) and heater regulator. The heater was connected to six tubes with a diameter of 19.05 mm and height of 65.8 mm, with each tube having the same power. Total heating power of 40 W was applied to the six tubes using a regulator. The heating air flowing through the tubes occurs via convection. Thus, the air at the outlet side becomes hotter than that at the inlet side.

A pressure micromanometer (Fluke type 922, with an accuracy of ± 0.05) was used to monitor the flow pressure drop. Two pitot tubes, each set 26 cm ahead of the inlet of the test specimen and 2.5 cm behind it, were connected to a micromanometer to measure the pressure drop. The pressure drop measurements were recorded 30 times for 5 sek on at each speed variation. Furthermore, flow visualisation was performed by

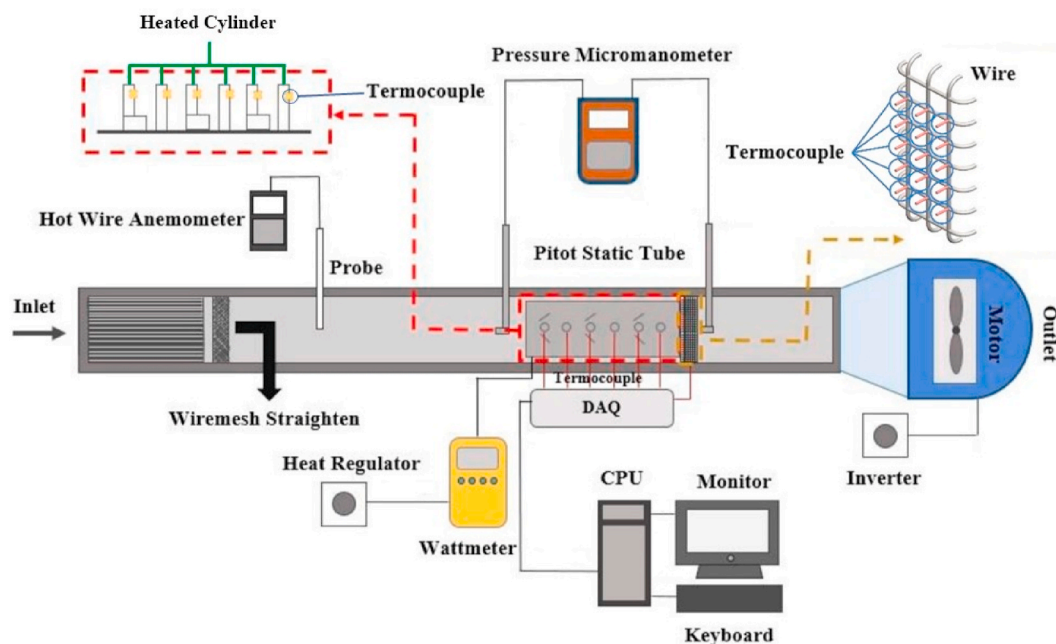


Fig. 1. Experimental tool schematic.

directing the smoke from vaporised fluid in the fluid vaporator into the mainflow.

The VGs used as test specimens were perforated rectangular winglet pair (PRWP) and perforated concave rectangular winglet pair (PCRWP) vortex generators (VGs). Perforated is a term for holes in the VGs, as shown in Fig. 2. The VGs have dimensions of the same length and width of 30 mm, with 36 holes. The bore diameter on the VGs was 2.5 mm. The distance between the holes was 5 mm from the center.

The VGs are placed on an aluminium plate measuring $500 \times 165 \times 1$ mm. The geometry and the pitch between VGs for both in-line and staggered configurations are shown in Fig. 3, with an angle of attack (α) of 150 [2]. The distance between the cylinders is 120 mm, with a cylinder diameter of 19.05 mm.

The VGs configurations were arranged in-line and staggered on the plate. The perforated rectangular winglet (PRW) and perforated concave rectangular winglet (PCRW) VGs in-line configurations with one, two and three pairs are shown in Fig. 4. For each pair, the VGs were placed

on the left and right sides of the first row of tubes. VGs were placed in the first- and third-row tubes for two pairs. For the three pairs, VGs were placed on the first-, third-, and fifth-row tubes.

The PRW and PCRW VGs staggered configurations with one, two, and three pairs are shown in Fig. 5. For one pair, the VGs are placed on the right side of the first-row tube and on the left side of the second. The VGs are placed on the right side of the first and third row tubes and on the left side of the second and fourth tubes for two pairs. For the three pairs, the VGs are placed on the right side of the first, third and fifth rows of the tubes and on the left side of the second, fourth and sixth tubes.

2.2. Parameter definitions

The parameters in this study were derived from the equation used by Oneissi et al. to obtain the thermal enhancement factor (TEF) [22].

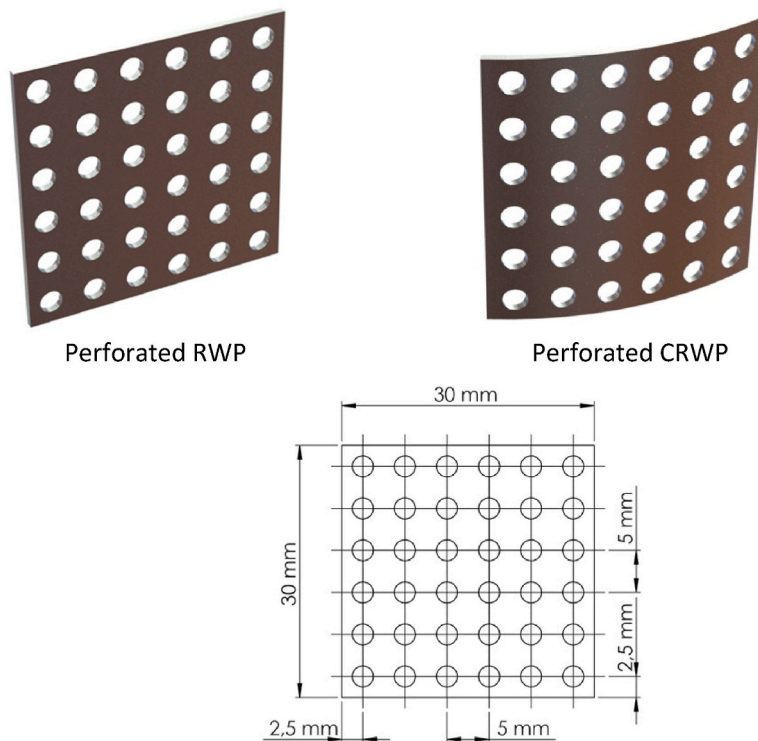


Fig. 2. Geometry of the VGs.

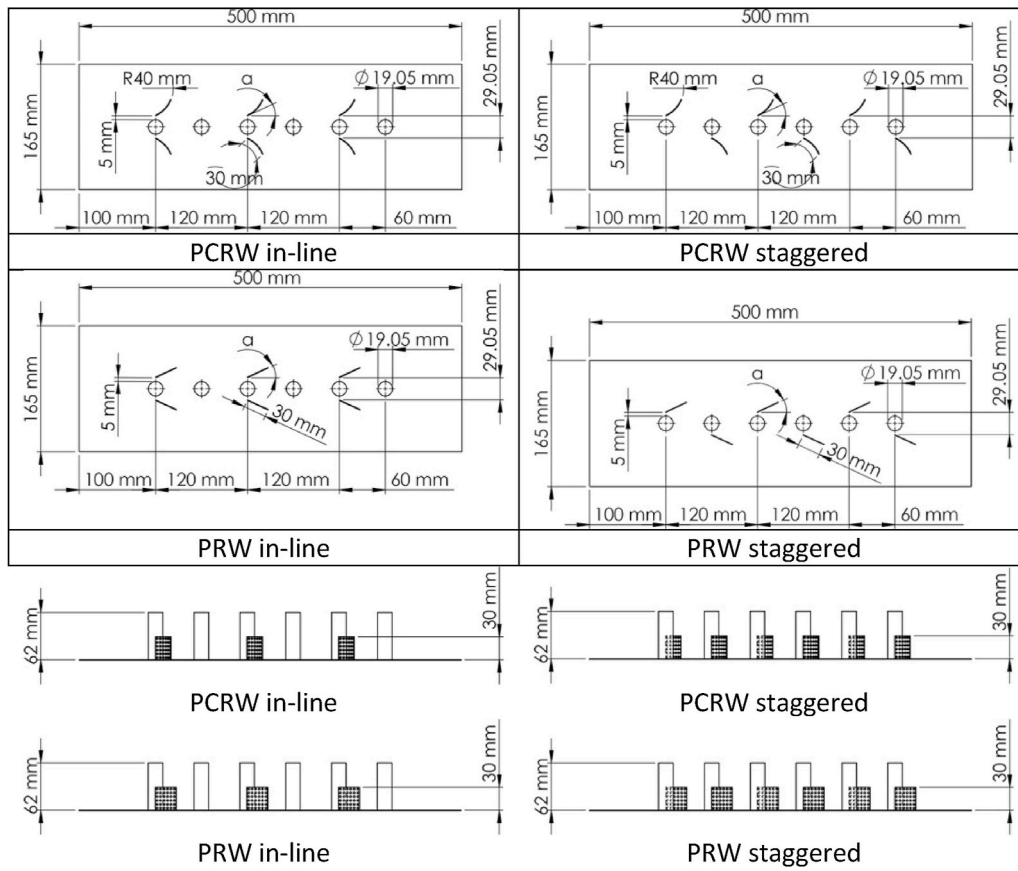


Fig. 3. Geometry and pitch of the VGs.

$$TEF = \frac{Nu}{Nu_0} \left(\frac{f}{f_0} \right)^{\frac{1}{3}} \quad (1)$$

The Nusselt number and friction factor for the baseline conditions are symbolised as (Nu_0) and (f_0) , and (Nu) and (f) based on the research of Zeeshan et al. [23]

$$Nu = \frac{q D_h}{A_{tube} \Delta T_{LMTD} k} \quad (2)$$

$$h = \frac{q}{A_{tube} \Delta T_{LMTD}} \quad (3)$$

$$q = \dot{m} c_p (T_{out} - T_{in}) \quad (4)$$

where D_h , A_{tube} , ΔT_{LMTD} , \dot{m} , c_p , T_{out} and T_{in} , are hydraulic diameter, tube surface area, log mean temperature difference, mass flow rate, specific heat, outlet temperature, and inlet temperature, respectively

$$D_h = \frac{4A_c}{p} = \frac{4ab}{2(a+b)} = \frac{2ab}{a+b} \quad (5)$$

$$\Delta T_{LMTD} = \frac{(\bar{T}_{tube} - \bar{T}_{out}) - (\bar{T}_{tube} - \bar{T}_{in})}{\ln[(\bar{T}_{tube} - \bar{T}_{out}) - (\bar{T}_{tube} - \bar{T}_{in})]} \quad (6)$$

where A_c and T_{tube} are channel surface area and tube temperature, respectively.

The result of D_h is used to calculate Re with the formula

$$Re = \frac{\rho u_{in} D_h}{\mu} \quad (7)$$

and friction factor (f) was determined to evaluate the performance of hydro dynamic using

$$f = \frac{2\Delta P D_h}{\rho V^2 (L + 6D)} \quad (8)$$

where ρ , V , and L are the air density, inlet airflow velocity and length of the test specimen, respectively.

The equation required to determine the cost-benefit ratio (CBR), defined as the ratio of pressure drop per variation in Nu number, as formulated by Tian et al. [25], is as follows:

$$CBR = \frac{\% \Delta P}{\% Nu} \quad (9)$$

This concept investigates whether the method used to enhance the heat-transfer rate is economically efficient. In the hydrodynamic test, the pressure drop (ΔP) is measured by the pressure difference on the sides of P_{inlet} and P_{outlet} of the test specimen in the tested part using equation (10):

$$\Delta P = P_{inlet} - P_{outlet} \quad (10)$$

2.3. Validation

The current study is a follow-up investigation to the work of Yafid et al. [24], and the experimental setup was similar to that of Yafid et al. The difference between the current study and the experiment of Yafid et al. is a test object in which the current study uses concave rectangular winglet (CRW) VGs; in Yafid et al.'s experiment concave delta winglet (CDW) VGs are used. Whitaker et al. [25] studied the heat transfer characteristics of airflow through a single cylinder in a rectangular duct. The results of Yafid et al. were valid, and the same experimental set-up was determined. The Nu value from the experiment of Yafid et al. were comparable with the Nu values from the experiments of Whitaker et al. in the Reynolds number (Re) range of 2143 to 11,763.

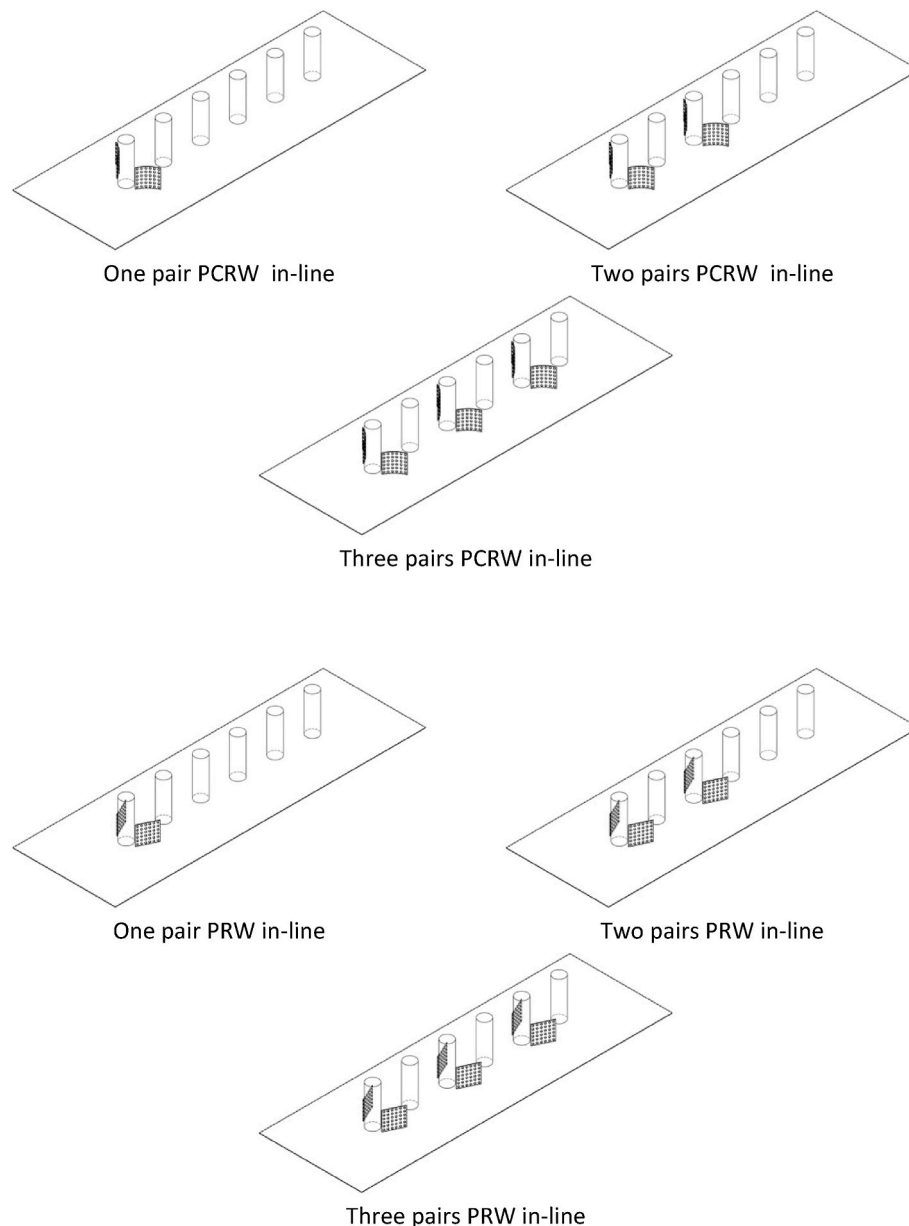


Fig. 4. VGs pairs in-line configurations.

3. Results and discussion

3.1. Flow visualisation

A flow visualisation test was performed to observe the longitudinal vortices (LV) formed after the flow passed through the VGs in the rectangular channel. This test was conducted under low-light conditions to clarify the LV. The laser beam was refracted by a cylindrical glass (diameter 5 mm), which produced a cross-sectional area perpendicular to the direction of the flow. Smoke formed from the evaporation of the liquid was used to visualise the LV in the flow. The VGs used in this visualisation test were PRWP and PCRWP with an in-line arrangement, as shown in Fig. 6.

In Fig. 6 (c) and (d), the PCRWP VGs appear to produce longitudinal vortices (LV) in a wide flow area compared with the PRWP VGs in Fig. 6 (a) and (b) downstream. The back region of the PCRWP VGs had a wider frontal surface area than the PRWP VGs. Consequently, mixing the near-fluid the channel walls with the fluid in the mainstream is better, meaning that the heat transfer rate is increased [26]. Downstream, the

LV compression in the wake area increases the fluid flow velocity passing through the cylindrical structure, thereby increasing the heat transfer rate from the channel surface to the fluid flow in the wake region [27]. The increase in heat transfer produced when using PCRWP VGs was better than that with PRWP VGs.

3.2. Perforated vortex generators effect on heat transfer

The increase in the convection heat transfer was due to the mixing of fluids caused by the strong longitudinal vortices (LVs) [28]. The strength of the LVs is caused by the amount of VGs sets; increasing the amount of VGs pairs in the test specimen can increase the coefficient of the convection heat transfer [29], as shown in Fig. 7.

In Fig. 7, we can see the convective heat transfer coefficient with respect to the Reynolds number (Re), analysed after installing the PCRWP and PRWP with pairs ranging from one, two and three, arranged in-line or staggered. Based on Fig. 7, the convective heat transfer coefficient increased with a rise in Re due to an increase in flow vortices and high turbulence intensity in the channel [30], alongside a reduction in

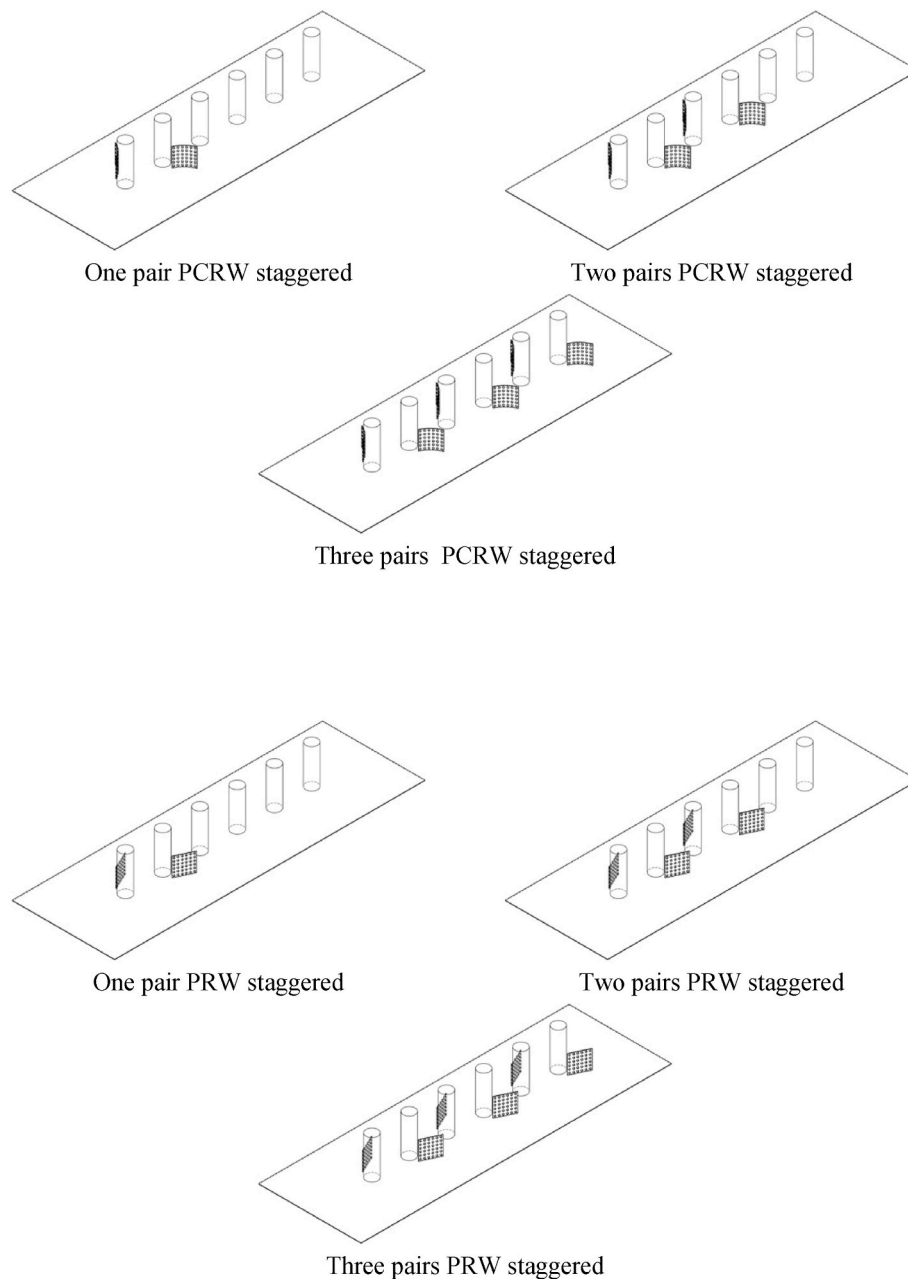


Fig. 5. VGs pairs staggered configurations.

the wake region and stagnation area for each increase in flow velocity [31]. The improve in heat transfer for the staggered was better than that for the PCRW VGs with any number of pairs at the highest Re (11,000). The results in Fig. 7 show that the PCRWP VGs worked better than the PRWP VGs, and the staggered arrangement of the former, with three pairs, gave the highest yield ($153.5 \text{ W/m}^2 \cdot \text{K}$), as shown in Fig. 7(c). Two PCRW pairs ($137.33 \text{ W/m}^2 \cdot \text{K}$, Fig. 7(b)) were better than one ($132.25 \text{ W/m}^2 \cdot \text{K}$) (Fig. 7(a)) because the VGs with a concave surface destabilise the force of centrifugal of the fluid flow, strengthening the flow vortices and making the mixing of the hot fluid near the wall with the cold fluid of the main flow more robust [32]. In Fig. 7(a), the convection heat-transfer coefficient for the case of the in-line PRW VGs has the same value as that of the in-line or staggered PCRW VGs in a pair of VGs. In one pair of VGs, a longitudinal vortex is generated after the flow hits and weakens the VGs [29]. This result contrasts with the cases with two and three pairs of VGs, where the longitudinal vortex produced after striking the first VGs is amplified again when the flow strikes the second

VGs and so on. Therefore, the value of the heat transfer coefficient in the case of a pair of PRW VGs is the same value as that of PCRW VGs at Reynolds numbers above 8000.

3.3. Effect of perforated vortex generators on pressure drop

Using VGs can affect the increase in heat transfer, but there is often an accompanying increase in pressure drop, as shown in Fig. 8, where an increase in pressure drop can be seen along with the increases in Re and pair numbers for both the VG types PCRW and PRW. In general, the highest pressure drop was observed using the PCRWP VGs with a staggered configuration for all Re , except for one pair of VGs. The highest pressure drop was found in the PRWP VGs with an in-line configuration at Re greater than 8000. The pressure drop on the staggered VGs was found to be higher than that on the in-line configuration because of the shorter distance between the VGs of the staggered configuration than that of the in-line [29], caused by the resistance of fluid flow against the

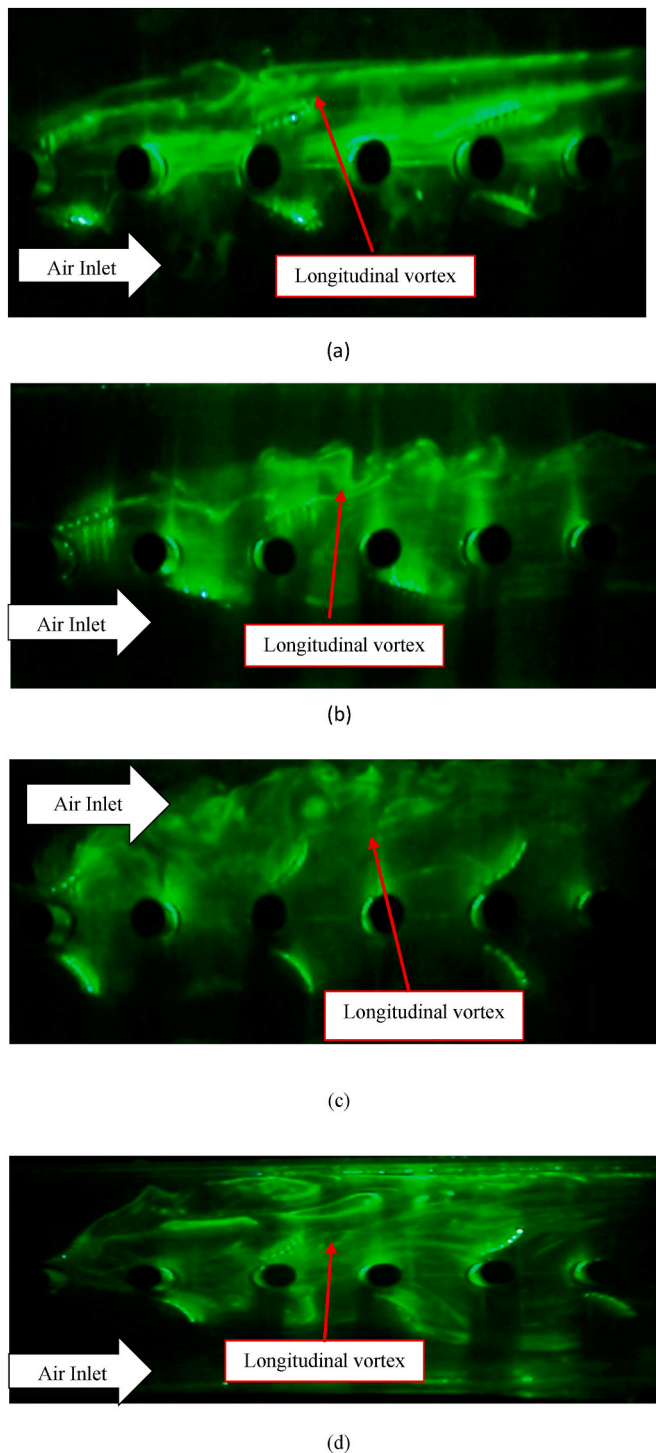


Fig. 6. Visualisation of LV generated by (a) in-line PRWP, (b) staggered PRWP, (c) in-line PCRWP and (d) staggered PCRWP.

walls of the VGs and the expansion of the frontal zone of the VGs in the next-pair arrangement [33]. The pressure drop in the staggered arrangement was lower than that in the in-line arrangement, whereas the PRW VGs type created a lower pressure drop than the PCRW VGs because the latter reduced the frontal area hit by the airflow, resulting in a decrease in drag [34]. In addition, the jet flow from the VG hole can reduce the stagnation flow, which can reduce the pressure drop [35]. A significant decrease in the pressure drop was due to the VG perforation [36]. The best pressure drop value for one pair with a staggered arrangement was 4.58 Pa (see Fig. 4(a)), whereas two pairs (5 Pa, Fig. 4

(b)) were better than three (5.4 Pa, Fig. 4(c)).

3.4. Effect of perforated VGs on thermal enhancement factor

TEF exhibited the hydraulic thermal performance while using VGs, which played a role in restructuring the incoming fluid flow pattern. The increase in the TEF was due to the influence of complex overlapping structures, which meant that the flow developed into a turbulent structure, significantly affecting the heat transfer increase [37]. The experimental TEF values are shown in Fig. 9.

The TEF is the thermal-hydraulic performance which is the ratio of the increase in heat transfer to the pressure drop ratio. In general, the highest TEF was observed when the PCRWP VGs were used with a staggered configuration, as depicted in Fig. 9. The PCRW creates wider flow vortices that can reduce the wake area behind the cylinder. Reducing the wake area can reduce the recirculation zone, affecting the heat transfer from the back of the cylinder to the stream [26]. A large-radius, high-intensity anterior-posterior vortex can reduce the wake area. A lessening within the wake zone increased the flow velocity behind the tube and reduced the recirculation area, resulting in increased heat transfer in this area [27,38]. As shown in Fig. 9, there was an increase in the TEF with greater pairs of VGs used for both the PCRW and PRW VG because the PCRW produced wider flow vortices, which reduced the wake region behind the cylinder, thereby reducing the recirculation zone and impacting the heat transfer increment from the rear cylinder surface to the stream [39]. In this process, a large number of longitudinal vortices with high intensities can reduce the wake area, which increases the flow velocity downstream of the tube and reduces the recirculation region, leading to an increased heat-transfer rate in the region [40,41]. Based on Fig. 9, the best TEF increase occurred at Re between 8000 and 9000. The best TEF values, with one, two and three pairs occurred in the staggered arrangement with PCRW VGs, at 1.18, 1.20 and 1.29, respectively (see Fig. 9).

3.5. Effects of perforated VGs on the cost-benefit ratio

Economic evaluation cannot be conducted based only on the TEF and the net profit from the heat load of the transferred unit [26]. Instead, it must be determined by evaluating the economic value of the heat-transfer improvement by calculating the cost benefit ratio (CBR), as shown in Fig. 10.

Fig. 10 show the result of the CBR calculation to compare the percentage increase in the pressure drop with the percentage increase in the Nusselt number when using VGs. These results indicate that a lower CBR improves thermal performance, which is greater than the drag force [25]. The greatest increase in CBR occurred with the PRW VGs, with an in-line arrangement, totalling 4.57, 4.95 and 3.56 for one, two and three pairs, respectively. The lowest CBR was measured when three sets of PCRW vortex generators with a staggered arrangement were used. The lowest CBR were obtained with the three pairs of staggered-type VGs PCRW. The three VG pairs showed a lower CBR than the one and two pairs because they resulted in the greatest increase in the Nusselt number, accompanied by a lower pressure drop increase, which lowered the CBR. These results show that a lower CBR improves thermal performance relative to resistivity [26]. A low value CBR indicates a more economical value using VGs. In general, using PCRWP VGs with a staggered configuration is the best.

3.6. Heat loss analysis

Heat loss analysis was performed by considering the convection heat transfer from the six tubes to the surrounding fluid flow. The heat transfer rate was calculated for laminar and turbulent flows.

The heat loss in this experiment was calculated by calculating the difference between the induced electric power and total heat through convection from the surface of the tubes to the fluid. In this experiment,

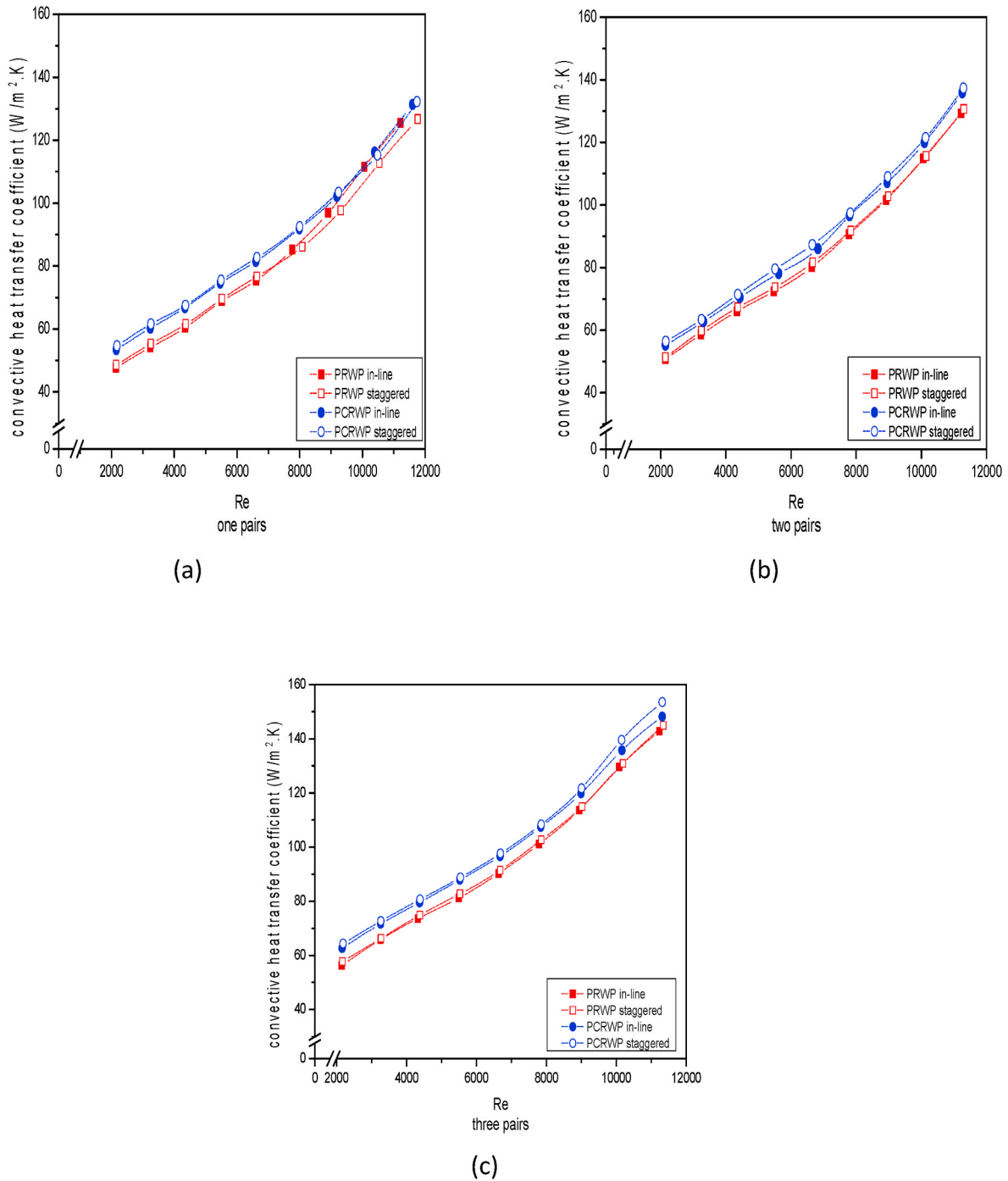


Fig. 7. Graphs of convective heat-transfer coefficient against Reynolds number: (a) one, (b) two and (c) three pairs.

six tubes in a wind tunnel were heated using a heater at a power of 40 W; the velocity of the inlet fluid is varied from 0.4 to 2 m/s at intervals of 0.2 m/s or in the Reynolds number range from 2143 to 11,763. Based on the Reynolds number range, two types of flows were determined; laminar and turbulent. Therefore, the heat loss was determined from the correlation between laminar at 0.4 m/s and turbulent for other velocities. The experimental data for the hydraulic diameter D_h , tube surface area A_{tube} , channel surface area A_c and air specific heat c_p are 0.09223 m, 0.02338908 m², 0.01056 m² and 1.007 J/kgK, respectively. Table 1 is a baseline for calculating heat loss

From Table 1, the greater the velocity with an increase in the Re , the lower the heat loss. It can be observed that the heat flow from the heater not only spreads into the tube, but convection also occurs outside the

tube. The heat output increased with Re , i.e., the higher the flow velocity, the greater the turbulence through the cylinder and the higher the turbulence intensity. An increase in the turbulence intensity between a cold airflow and hot cylinder with a constant surface temperature is caused by the airflow velocity [26]. In row-tube arrays, this recirculation area increased for the second and subsequent columns. A lower air velocity in the circulation region indicated less airflow in the region participating in the local heating process [37]. The heat loss under all conditions in this experiment is listed in Table 2.

Table 2 shows that the lowest heat loss occurs when three sets of PCRWPs are staggered. The placement of the VGs can increase heat transfer in square ducts as the VGs create longitudinal vortices, which in turn increase vortex strength in the wake region downstream of the tube.

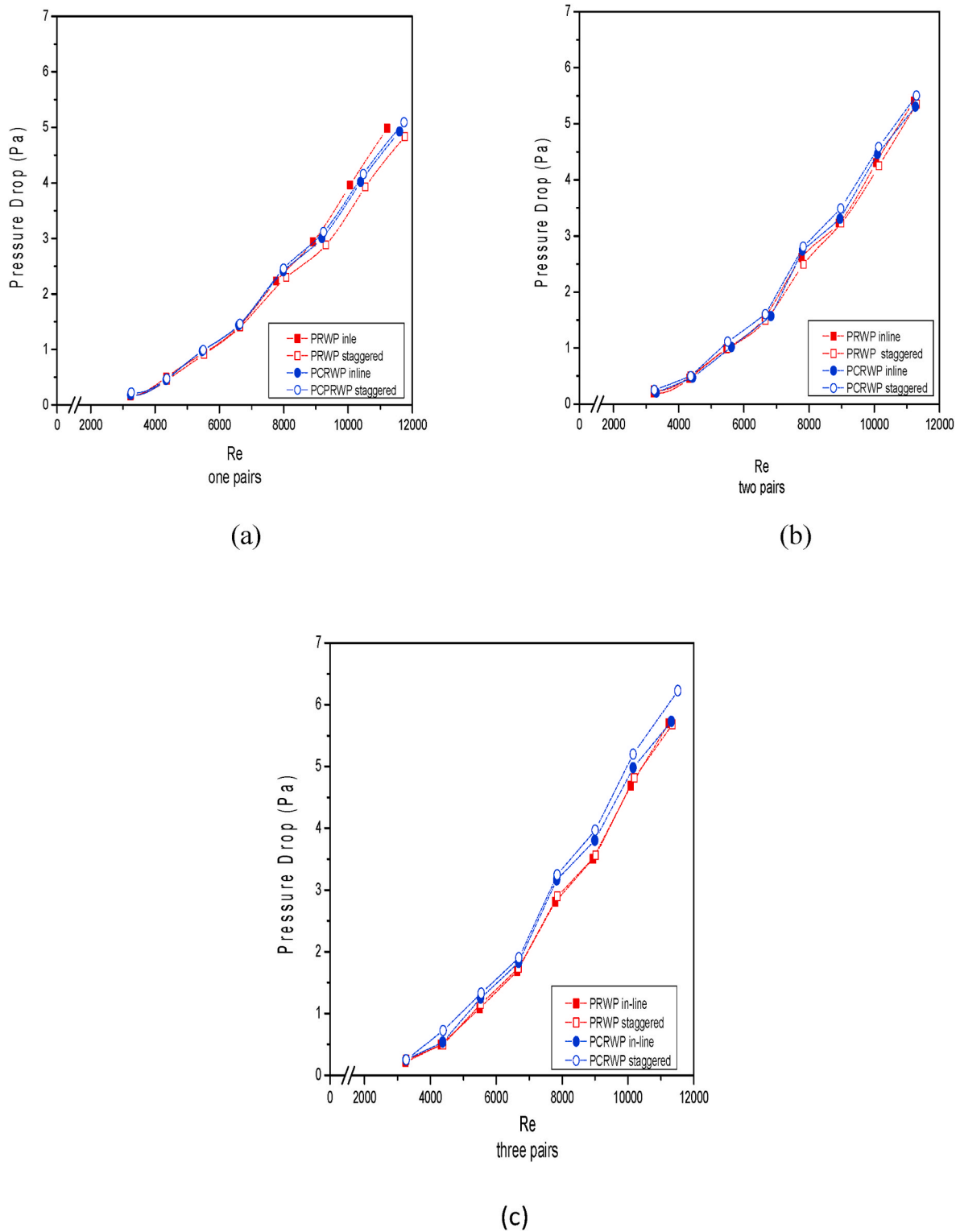


Fig. 8. Graph of pressure drop against Reynolds number: (a) one, (b) two and (c) three pairs.

Longitudinal vortices make the overall temperature field more uniform, improve heat mixing and boundary layer modification, and improve heat transfer performance. A higher number of vortex generators creates more longitudinal vortices and significantly increases heat transfer [26, 29].

3.7. Uncertainty analysis

In this section, uncertainty analysis calculation data will be shown for the temperature at base-line conditions with a velocity of 0.4 m/s as shown in Table 3.

From these data, it is found that \bar{T}_{Tube} can be calculated by the equation as

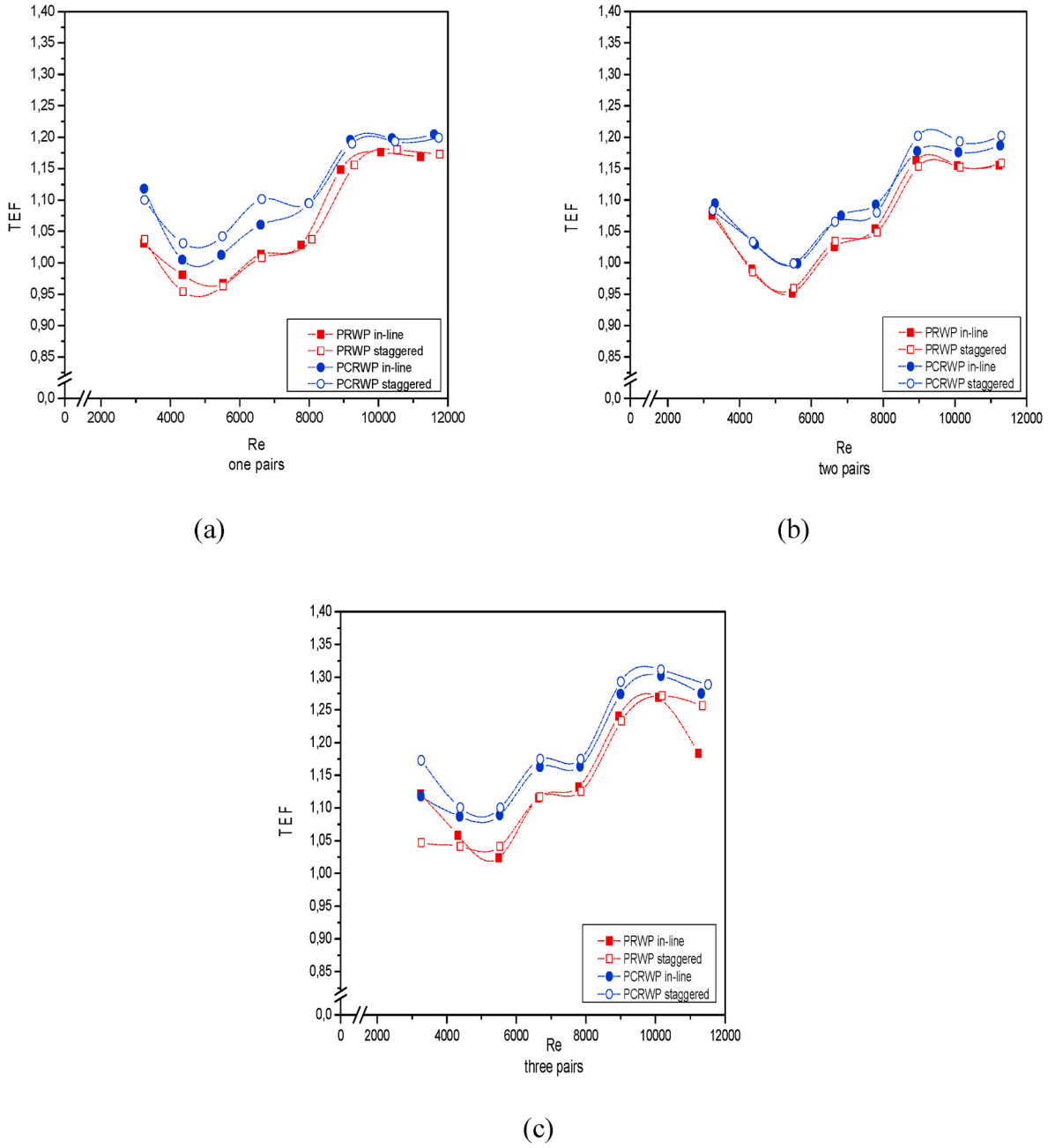


Fig. 9. Graph of thermal enhancement factor against Reynolds number: (a) one, (b) two and (c) three pairs.

$$\bar{T}_{Tube} = \frac{\bar{T}_{Tube1} + \bar{T}_{Tube2} + \bar{T}_{Tube3} + \bar{T}_{Tube4} + \bar{T}_{Tube5} + \bar{T}_{Tube6}}{6} = 49.56^{\circ}\text{C} \quad (11)$$

Then, the average standard deviation is obtained by the following formula.

$$s_{tube} = \sqrt{\frac{\sum_{i=1}^N (T_{tubei} - \bar{T}_{tube})^2}{N(N-1)}} = 0.029 \quad (12)$$

Therefore, the average T_{tube} can be written as $49.5 \pm 0.029^{\circ}\text{C}$. \bar{T}_{out} calculation results obtained 32.95°C . The average standard deviation was calculated using the following equation:

$$s_{Tout} = \sqrt{\frac{\sum_{i=1}^N (T_{outi} - \bar{T}_{out})^2}{N(N-1)}} = 0.051 \quad (13)$$

Furthermore, the average value of T_{out} can be written as $32.95 \pm$

0.051°C . Using the same equation, the standard deviation of T_{in} was found to be 0.033. Thus, the average T_{in} value was $29.75 \pm 0.016^{\circ}\text{C}$.

The value of q at a speed of 0.4 m/s was found to be 19.48 W. To determine of the standard deviation of q , the following equation was used:

$$RSS_q = \sqrt{\left(s(\Delta T_{out}) \frac{\partial q}{\partial T_{out}}\right)^2 + \left(s(\Delta T_{in}) \frac{\partial q}{\partial T_{in}}\right)^2} \quad (14)$$

$$\frac{\partial q}{\partial T_{out}} = \frac{\partial(m \cdot c_p \cdot T_{out} - m \cdot c_p \cdot T_{in})}{\partial T_{out}} = m \cdot c \cdot p$$

$$\frac{\partial q}{\partial T_{in}} = \frac{\partial(m \cdot c_p \cdot T_{out} - m \cdot c_p \cdot T_{in})}{\partial T_{in}} = -(m \cdot c \cdot p)$$

where $s(\Delta T_{out}) = 0.051^{\circ}\text{C}$ and $s(\Delta T_{in}) = 0.033^{\circ}\text{C}$, ensuring, that $RSS_q =$

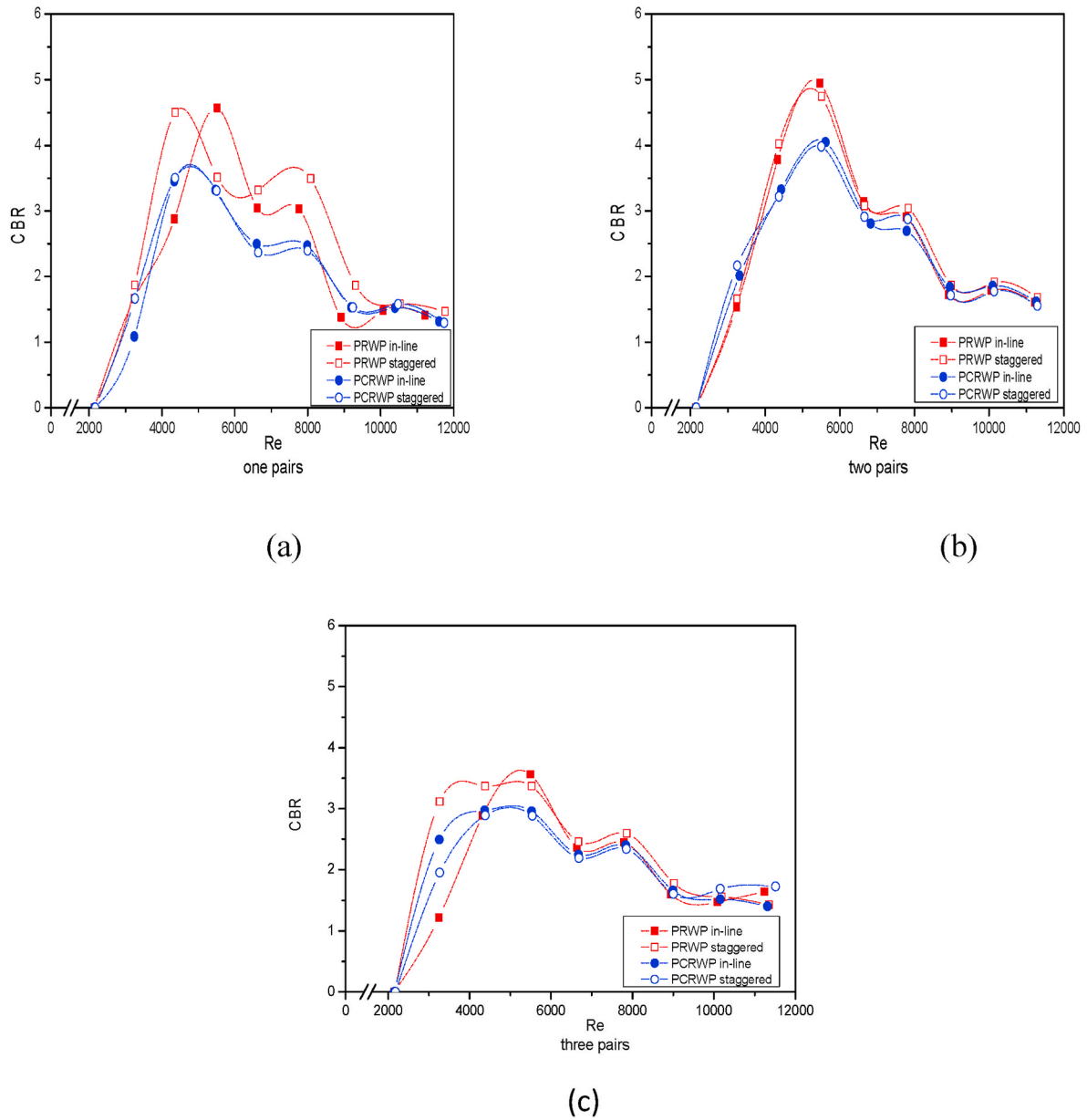


Fig. 10. Graph of cost-benefit ratio against Reynolds number: (a) one, (b) two and (c) three pairs.

± 0.290 W. Therefore, the heat transfer rate q becomes 19.48 ± 0.290 W. The value of ΔT_{lmd} at a speed of 0.4 m/s was found to be 18.56 °C. To determine the value of the standard deviation of ΔT_{lmd} we used the following equation:

$$\frac{\partial(\Delta T_{lmd})}{\partial T_{out}} = \frac{\partial \left(\frac{(T_{tube} - T_{out}) - (T_{tube} - T_{in})}{\ln \frac{T_{tube} - T_{out}}{T_{tube} - T_{in}}} \right)}{\partial T_{out}}$$

$$RSS_{\Delta T_{lmd}} = \sqrt{\left(s(\Delta T_{tube}) \frac{\partial(\Delta T_{lmd})}{\partial T_{tube}} \right)^2 + \left(s(\Delta T_{out}) \frac{\partial(\Delta T_{lmd})}{\partial T_{out}} \right)^2 + \left(s(\Delta T_{in}) \frac{\partial(\Delta T_{lmd})}{\partial T_{in}} \right)^2} \quad (15)$$

$$\frac{\partial(\Delta T_{lmd})}{\partial T_{tube}} = \frac{\partial \left(\frac{(T_{tube} - T_{out}) - (T_{tube} - T_{in})}{\ln \frac{T_{tube} - T_{out}}{T_{tube} - T_{in}}} \right)}{\partial T_{tube}}$$

$$\frac{\partial(\Delta T_{lmd})}{\partial T_{in}} = \frac{\partial \left(\frac{(T_{tube} - T_{out}) - (T_{tube} - T_{in})}{\ln \frac{T_{tube} - T_{out}}{T_{tube} - T_{in}}} \right)}{\partial T_{in}}$$

Table 1
Heat loss baseline.

	v (m/s)	Re	Mass flow rate (kg/s)	Density (kg/m ³)	Dynamics viscous (kg/ms)	k	Pr	T inlet (C)	T outlet (C)	T tube (C)	ΔT LMTD	ΔT (T tube - T inlet)	Nu	h (W/mK)	q conv (W)	q input (W)	q loss (W)
baseline	0.4	2165	0.004757	1.13	1.9.E-05	0.03	0.73	29	33	50	19	21	155	45	19.48	40	20.52
	0.6	3291	0.00719	1.13	1.9.E-05	0.03	0.73	28	31	46	16	18	174	50	18.98	40	21.02
	0.8	4413	0.009618	1.14	1.9.E-05	0.03	0.73	28	30	44	15	16	192	50	19.19	40	20.81
	1	5545	0.012056	1.14	1.9.E-05	0.03	0.73	28	30	43	14	15	214	55	19.84	40	20.16
	1.2	6661	0.014477	1.14	1.9.E-05	0.03	0.73	28	29	43	14	15	228	61	21.15	40	18.85
	1.4	7826	0.016958	1.15	1.9.E-05	0.03	0.73	28	29	41	12	13	247	70	20.30	40	19.70
	1.6	8965	0.019407	1.15	1.9.E-05	0.03	0.73	27	29	40	12	13	263	75	21.03	40	18.97
	1.8	10,110	0.021863	1.15	1.9.E-05	0.03	0.73	27	28	39	12	12	296	84	22.54	40	17.46
	2	11,272	0.024341	1.15	1.9.E-05	0.03	0.73	27	28	38	11	11	342	97	24.17	40	15.83

Table 2

Calculation of heat loss for the whole case.

type VGs	q conv (W)	q input (W)	q loss (W)
Baseline	20.74	40	19.26
PCRWPI1	25.15	40	14.85
PCRWPI2	27.55	40	12.45
PCRWPI3	27.61	40	12.39
PCRWPS1	26.43	40	13.57
PCRWPS2	26.43	40	13.57
PCRWPS3	27.94	40	12.06
PRWPI1	24.09	40	15.91
PRWPI2	27.25	40	12.75
PRWPI3	28.82	40	11.18
PRWPS1	23.94	40	16.06
PRWPS2	26.37	40	13.63
PRWPS3	28.12	40	11.88

Table 3

Base-line test temperature data at a speed of 0.4 m/s.

T (Tube ₁)	T (Tube ₂)	T (Tube ₃)	T (Tube ₄)	T (Tube ₅)	T (Tube ₆)
49.19093	51.21368	48.32313	49.76915	47.80219	51.27142
49.1834	51.17728	48.3156	49.79053	47.7657	51.2639
49.14545	51.16826	48.30655	49.7526	47.7856	51.25489
49.12105	51.17277	48.28214	49.72821	47.76118	51.2594
49.15297	51.20465	48.28515	49.73122	47.73524	51.2624
49.09966	51.15141	48.28967	49.73573	47.76871	51.26691
49.09815	51.14991	48.23029	49.73423	47.73826	51.29428
49.08912	51.14089	48.25019	49.66739	47.72922	51.22751

where $s(\Delta T_{tube}) = 0.029^\circ\text{C}$, $s(\Delta T_{out}) = 0.051^\circ\text{C}$ and $s(\Delta T_{in}) = 0.033^\circ\text{C}$; we get $RSS_{\Delta T_{lmd}}$ of ± 0.043 , ensuring, that the obtained ΔT_{lmd} is 8.56 ± 0.043 .

The value of Nu at a speed of 0.4 m/s was found to be 155.31. The standard deviation of Nu was obtained using following equation

$$RSS_{Nu} = \sqrt{\left(s(q) \frac{\partial Nu}{\partial Q}\right)^2 + s(\Delta T_{lmd}) \frac{\partial Nu}{\partial \Delta T_{lmd}}} \quad (16)$$

$$\frac{\partial Nu}{\partial q} = \frac{\partial(q \cdot D_h \cdot At^{-1} \cdot \Delta T_{lmd}^{-1} \cdot k^{-1})}{\partial q} = \frac{D_h}{(At)(\Delta T_{lmd})(k)}$$

$$\frac{\partial Nu}{\partial \Delta T_{lmd}} = \frac{\partial(q \cdot D_h \cdot At^{-1} \cdot \Delta T_{lmd}^{-1} \cdot k^{-1})}{\partial \Delta T_{lmd}} = \frac{q \cdot D_h}{(At)(\Delta T_{lmd})^2(k)}$$

With the values of $s(q) = 0.290 \text{ W}$ and $s(\Delta T_{lmd}) = 0.043$, the obtained RSS_{Nu} was $\pm 2.889 \text{ W/(m}^2\text{C)}$. Therefore, the value of RSS_{Nu} is $155.31 \pm 2.889 \text{ W/m}^2\text{C}$.

The value of h at a speed of 0.4 m/s was found to be 44.86. To determine the standard deviation of Nu the following equation is used

$$RSS_h = \sqrt{\left(s(Nu) \frac{\partial h}{\partial Nu}\right)^2} \quad (17)$$

$$\frac{\partial h}{\partial Nu} = \frac{\partial(h \cdot D_h \cdot k^{-1})}{\partial h} = \frac{k}{D_h}$$

Furthermore, the value of D_h is 0.092 m and k at $T_f = 40.24$ is 0.026. So the value of h at a speed of 0.4 m/s is:

$$RSS_h = \sqrt{\left(s(Nu) \frac{\partial h}{\partial Nu}\right)^2} = 0.83$$

Thus, the number h at a speed of 0.4 m/s is 44.86 ± 0.83 . So, the error h for the baseline at a speed of 0.4 m/s is

$$Error = \frac{RSS_h}{h} \times 100 \quad (18)$$

Table 4

Baseline pressure drop data at a speed of 2.0 m/s.

ΔP (Pa)			
Data to	2.0 m/s	Data to	2.0 m/s
1	0.013	16	0.012
2	0.013	17	0.013
3	0.013	18	0.012
4	0.013	19	0.012
5	0.012	20	0.013
6	0.013	21	0.013
7	0.013	22	0.012
8	0.012	23	0.013
9	0.013	24	0.012
10	0.013	25	0.013
11	0.013	26	0.013
12	0.013	27	0.013
13	0.012	28	0.013
14	0.012	29	0.012
15	0.013	30	0.012

$$Error = \frac{0.83}{44.86} \times 100 = 1.51\%$$

From the test in the baseline case with a speed of 2.0 m/s, the results of the pressure drop are listed in Table 4, which show that the average P can be calculated as follows:

$$\overline{\Delta P} = \frac{\Delta P_1 + \Delta P_2 + \Delta P_3 + \dots + \Delta P_{30}}{30} = 3.51 \text{ Pa} \quad (19)$$

The average standard deviation of the pressure drop can then be calculated using the equation

$$s = \sqrt{\frac{\sum_{i=1}^N (\Delta P_i - \overline{\Delta P})^2}{N(N-1)}} = 8.9 \times 10^{-5} \quad (20)$$

Baseline case for the pressure drop value at a speed of 2.0 m/s is $3.51 \pm 8.9 \times 10^{-5}$ Pa. Then, the error in the form of percentage can be calculated using the following equation:

$$\frac{8.9 \times 10^{-5}}{3.51} \times 100 = 0.71$$

The equal calculation approach changed into used for all data. Therefore, the overall error outputs for the pressure-drop vortex generator with placement variations (in-line and staggered), Re and amount of VG sets (one, two and three) are listed in Table 5.

The average TEF results from the experimental results can be calculated as follows.

$$\overline{TEF} = \frac{TEF_1 + TEF_2 + TEF_3 + \dots + TEF_{12}}{12} = 1.12 \quad (21)$$

Then, the average standard deviation of the TEF can be calculated with the equation

Table 5Overall pressure drop (ΔP).

Vortex Generator Variations	Overall Error P (perforated)
1 PRWP in-line	2.94%
2 PRWP in-line	2.87%
3 PRWP in-line	1.98%
1 PRWP staggered	2.88%
2 PRWP staggered	2.34%
3 PRWP staggered	1.36%
1 PCRWP in-line	2.72%
2 PCRWP in-line	1.80%
3 PCRWP in-line	1.80%
1 PCRWP staggered	2.43%
2 PCRWP staggered	1.91%
3 PCRWP staggered	0.97%

Table 6Overall error TEF .

Variasi Vortex Generator	Overall Error TEF (Berlubang)
1 RWP in-line	0.47%
2 RWP in-line	0.47%
3 RWP in-line	0.43%
1 RWP staggered	0.47%
2 RWP staggered	0.47%
3 RWP staggered	0.43%
1 CRWP in-line	0.45%
2 CRWP in-line	0.45%
3 CRWP in-line	0.42%
1 CRWP staggered	0.45%
2 CRWP staggered	0.45%
3 CRWP staggered	0.41%

$$s = \sqrt{\frac{\sum_{i=1}^N (TEF_i - \overline{TEF})^2}{N(N-1)}} = 1.07 \quad (22)$$

Therefore, the TEF value was 1.12 ± 1.07 . Then, the error in the form of percentage can be calculated using the following equation:

$$\frac{1.07}{1.12} \times 100 = 0.94\%$$

The overall error results for the TEF vortex generator with placement variations (in-line and staggered), Re and amount of VG sets (one, two and three) are listed in Table 6.

First, find the average CBR of the experimental results with the following formula.

$$\overline{CBR} = \frac{CBR_1 + CBR_2 + CBR_3 + \dots + CBR_{12}}{12} = 2.14 \quad (23)$$

The average standard deviation of the pressure drop CBR can then be calculated using the following equation:

$$s = \sqrt{\frac{\sum_{i=1}^N (CBR_i - \overline{CBR})^2}{N(N-1)}} = 1.60 \quad (24)$$

The CBR value is 2.14 ± 1.60 . Then the error in the form of percentage can be calculated using the following equation:

$$\frac{1.60}{2.14} \times 100 = 0.63\%$$

The overall error results for the CBR vortex generator with placement variations (in-line and staggered), Re and amount of VG sets (one, two and three) are listed in Table 7.

4. Conclusion

Based on the experimental results for perforated concave rectangular winglet pair vortex generators (PCRWP VGs) used to increase the heat transfer of airflow through heated tubes arranged in-line in the duct, we

Table 7Overall error CBR .

Variasi Vortex Generator	Overall Error CBR (Berlubang)
1 RWP in-line	0.32%
2 RWP in-line	0.29%
3 RWP in-line	0.45%
1 RWP staggered	0.32%
2 RWP staggered	0.31%
3 RWP staggered	0.45%
1 CRWP in-line	0.4%
2 CRWP in-line	0.42%
3 CRWP in-line	0.56%
1 CRWP staggered	0.43%
2 CRWP staggered	0.42%
3 CRWP staggered	0.66%

conclude that using PCRWP VGs affects the convection heat transfer coefficient, pressure drop in achieving hydraulic thermal performance and cost-benefit ratio. In our investigation, the best heat-transfer convection coefficient was $153.5 \text{ W/m}^2 \cdot \text{K}$ for the three pairs of PCRW VGs, in a staggered manner. The greatest improvement in the pressure drop value (4.58 Pa), occurred for one pair of PCRW VGs arranged in a staggered manner, whereas the hydraulic thermal performance was the best (1.29) in this experiment with the three pairs of PCRW VGs arranged in a staggered manner. Finally, the best CBR (3.56) was recorded for the three pairs of PCRW VGs composed in a staggered manner.

Credit author statement

Oktarina Heriyani: Conceptualization, Methodology, Investigation, Writing – original draft preparation.; Mohammad Djaeni: Supervision – Reviewing and Editing.; Syaiful: Conceptualization, Writing – Reviewing and Editing, Conceptualization.; Aldila Kurnia Putri: Visualisation, Validation.

Declaration of competing interest

The authors declare that they have no known competing financial interests or personal relationships that could have appeared to influence the work reported in this paper.

Acknowledgements

The authors would like to thank LEMLITBANG UHAMKA which has funded this research through internal grants from UHAMKA and UPPI UHAMKA what have contributed in facilitating translation and proof reading. The authors also thank the UNDIP thermofluidics laboratory, where the authors carried out this experiment.




References

- [1] R. Sebayang, AC Akan jadi pengkonsumsi listrik utama di Dunia, CNBC Indonesia (2018).
- [2] Z. Qian, Q. Wang, J. Cheng, Analysis of heat and resistance performance of plate fin-and-tube heat exchanger with rectangle-winglet vortex generator, *Int. J. Heat Mass Tran.* 124 (2018) 1198–1211, <https://doi.org/10.1016/j.ijheatmasstransfer.2018.04.037>.
- [3] D. Mugisidi, O. Heriyani, P.H. Gunawan, D. Apriani, Performance improvement of a forced draught cooling tower using a vortex generator, *CFD Lett.* 13 (1) (2021) 45–57, <https://doi.org/10.37934/cfdl.13.1.4557>.
- [4] A.J. Modi, N.A. Kalel, M.K. Rathod, Thermal performance augmentation of fin-and-tube heat exchanger using rectangular winglet vortex generators having circular punched holes, *Int. J. Heat Mass Tran.* 158 (2020) 1–16, <https://doi.org/10.1016/j.ijheatmasstransfer.2020.119724>.
- [5] K.W. Song, T. Tagawa, The optimal arrangement of vortex generators for best heat transfer enhancement in flat-tube-fin heat exchanger, *Int. J. Therm. Sci.* (2018), <https://doi.org/10.1016/j.jthermalsci.2018.06.011>.
- [6] C. Yu, H. Zhang, M. Zeng, R. Wang, B. Gao, Numerical study on turbulent heat transfer performance of a new compound parallel flow shell and tube heat exchanger with longitudinal vortex generator, *May 2019, Appl. Therm. Eng.* 164 (2020), 114449, <https://doi.org/10.1016/j.applthermaleng.2019.114449>.
- [7] M. Samadifar, D. Toghraie, Numerical simulation of heat transfer enhancement in a plate-fin heat exchanger using a new type of vortex generators, *September 2017, Appl. Therm. Eng.* 133 (2018) 671–681, <https://doi.org/10.1016/j.applthermaleng.2018.01.062>.
- [8] U. Kashyap, K. Das, B.K. Debnath, Effect of surface modification of a rectangular vortex generator on heat transfer rate from a surface to fluid, *August 2017, Int. J. Therm. Sci.* 127 (2018) 61–78, <https://doi.org/10.1016/j.jthermalsci.2018.01.004>.
- [9] U. Kashyap, K. Das, B.K. Debnath, Effect of surface modification of a rectangular vortex generator on heat transfer rate from a surface to fluid: an extended study, *August, Int. J. Therm. Sci.* 134 (2018) 269–281, <https://doi.org/10.1016/j.jthermalsci.2018.08.020>.
- [10] A.Q. Ibrahim, R.S. Alturahi, Experimental work for single-phase and two-phase flow in duct banks with vortex generators, *Sep, Results in Engineering* (2022), 100497, <https://doi.org/10.1016/j.rineng.2022.100497>.
- [11] K.W. Song, T. Tagawa, Z.H. Chen, Q. Zhang, Heat transfer characteristics of concave and convex curved vortex generators in the channel of plate heat exchanger under laminar flow, *November 2018, Int. J. Therm. Sci.* 137 (2019) 215–228, <https://doi.org/10.1016/j.jthermalsci.2018.11.002>.
- [12] K.A. Hammoodi, H.A. Hasan, M.H. Abed, A. Basem, A.M. Al-Tajer, Control of heat transfer in circular channels using oblique triangular ribs, *Sep, Results in Engineering* 15 (2022), 100471, <https://doi.org/10.1016/j.rineng.2022.100471>.
- [13] M. Zeeshan, S. Nath, D. Bhanja, A. Das, Numerical investigation for the optimal placements of rectangular vortex generators for improved thermal performance of fin-and-tube heat exchangers, *Appl. Therm. Eng.* (2018), <https://doi.org/10.1016/j.applthermaleng.2018.03.006>.
- [14] H. Linardos, G. Mavrogenis, D. Margaritis, Novel designs of LVGs conformations and introduction of Batch Heated and Channeled Pipe for increasing heat transfer efficiency in pipes, *Mar, Results in Engineering* 13 (2022), 100357, <https://doi.org/10.1016/j.rineng.2022.100357>.
- [15] O. Heriyani, M. Djaeni, Syaiful, Thermal-hydraulic performance analysis by means of rectangular winglet vortex generators in a channel: an experimental study, *European Journal of Engineering and Technology Research* 6 (3) (2021) 150–153, <https://doi.org/10.24018/ejers.2021.6.3.2424>.
- [16] C. Wang, Z. Wang, L. Wang, L. Luo, B. Sundén, Experimental study of fluid flow and heat transfer of jet impingement in cross-flow with a vortex generator pair, *Int. J. Heat Mass Tran.* 135 (2019) 935–949, <https://doi.org/10.1016/j.jheatmasstransfer.2019.02.024>.
- [17] Z. Sun, K. Zhang, W. Li, Q. Chen, N. Zheng, Investigations of the turbulent thermal-hydraulic performance in circular heat exchanger tubes with multiple rectangular winglet vortex generators, *Mar, Appl. Therm. Eng.* 168 (2020), 114838, <https://doi.org/10.1016/j.applthermaleng.2019.114838>.
- [18] P. Promvongse, S. Skullong, Thermo-hydraulic performance in heat exchanger tube with V-shaped winglet vortex generator, *Appl. Therm. Eng.* (2020), <https://doi.org/10.1016/j.applthermaleng.2019.114424>.
- [19] S. Skullong, P. Promthaisong, P. Promvongse, C. Thianpong, M. Pimsarn, Thermal performance in solar air heater with perforated-winglet-type vortex generator, *June, Sol. Energy* 170 (2018) 1101–1117, <https://doi.org/10.1016/j.solener.2018.05.093>.
- [20] Z. Han, Z. Xu, J. Wang, Numerical simulation on heat transfer characteristics of rectangular vortex generators with a hole, *Int. J. Heat Mass Tran.* 126 (2018) 993–1001, <https://doi.org/10.1016/j.jheatmasstransfer.2018.06.081>.
- [21] C. Luo, S. Wu, K. Song, L. Hua, L. Wang, Thermo-hydraulic performance optimization of wavy fin heat exchanger by combining delta winglet vortex generators, *Appl. Therm. Eng.* (2019), <https://doi.org/10.1016/j.applthermaleng.2019.114343>.
- [22] H. Naik, S. Tiwari, Effect of winglet location on performance of fin-tube heat exchangers with inline tube arrangement, *Int. J. Heat Mass Tran.* 125 (2018) 248–261, <https://doi.org/10.1016/j.jheatmasstransfer.2018.04.071>.
- [23] M. Zeeshan, S. Nath, D. Bhanja, A. Das, Numerical investigation for the optimal placements of rectangular vortex generators for improved thermal performance of fin-and-tube heat exchangers, *May, Appl. Therm. Eng.* 136 (2018) 589–601, <https://doi.org/10.1016/j.applthermaleng.2018.03.006>.
- [24] Y. Effendi, A. Prayogo, Syaiful, M. Djaeni, E. Yohana, Effect of perforated concave delta winglet vortex generators on heat transfer and flow resistance through the heated tubes in the channel, *Exp. Heat Tran.* 35 (5) (2022) 553–576, <https://doi.org/10.1080/08916152.2021.1919245>.
- [25] S. Whitaker, Forced Convection Heat Transfer Correlations for Flow In Pipes, Past Flat Plates, Single e Cylinders, Single Spheres, and for Flow In Packed Beds and Tube Bundles, Reprinted from, *AIChE J.* (1972).
- [26] M. Awais, A.A. Bhuiyan, Enhancement of thermal and hydraulic performance of compact finned-tube heat exchanger using vortex generators (VGs): a parametric study, *Jun, Int. J. Therm. Sci.* 140 (2019) 154–166, <https://doi.org/10.1016/j.jthermalsci.2019.02.041>.
- [27] A. Gupta, A. Roy, S. Gupta, M. Gupta, Numerical investigation towards implementation of punched winglet as vortex generator for performance improvement of a fin-and-tube heat exchanger, *Mar, Int. J. Heat Mass Tran.* 149 (2020), 119171, <https://doi.org/10.1016/j.jheatmasstransfer.2019.119171>.
- [28] M.W. Tian, S. Khorasani, H. Moria, S. Pourhedayat, H.S. Dizaji, Profit and efficiency boost of triangular vortex-generators by novel techniques, *Int. J. Heat Mass Tran.* 156 (2020), 119842, <https://doi.org/10.1016/j.jheatmasstransfer.2020.119842>.
- [29] Y.L. He, P. Chu, W.Q. Tao, Y.W. Zhang, T. Xie, Analysis of heat transfer and pressure drop for fin-and-tube heat exchangers with rectangular winglet-type vortex generators, *Nov, Appl. Therm. Eng.* 61 (2) (2013) 770–783, <https://doi.org/10.1016/j.applthermaleng.2012.02.040>.
- [30] M. Pranita Hendraswari, M.S. Tony, M.F. Soetanto, Heat Transfer Enhancement inside Rectangular Channel by Means of Vortex Generated by Perforated Concave Rectangular Winglets, 2021, <https://doi.org/10.3390/fluids6010043>.
- [31] A. R. Siwi Syaiful, T.S. Utomo, Y. Yurianto, R. Wulandari, Numerical analysis of heat and fluid flow characteristics of airflow inside rectangular channel with presence of perforated concave delta winglet vortex generators, *International Journal of Heat and Technology* 37 (4) (2019) 1059–1070, <https://doi.org/10.18280/IJHT.370415>.
- [32] A. Sinha, H. Chattopadhyay, A.K. Iyengar, G. Biswas, Enhancement of heat transfer in a fin-tube heat exchanger using rectangular winglet type vortex generators, *Oct. Int. J. Heat Mass Tran.* 101 (2016) 667–681, <https://doi.org/10.1016/j.jheatmasstransfer.2016.05.032>.
- [33] H. Ke, et al., Thermal-hydraulic performance and optimization of attack angle of delta winglets in plain and wavy finned-tube heat exchangers, *Mar, Appl. Therm. Eng.* 150 (2019) 1054–1065, <https://doi.org/10.1016/j.applthermaleng.2019.01.083>.

- [34] A. Arora, P.M.V. Subbarao, R.S. Agarwal, Development of parametric space for the vortex generator location for improving thermal compactness of an existing inline fin and tube heat exchanger, *Apr. Appl. Therm. Eng.* 98 (2016) 727–742, <https://doi.org/10.1016/J.APPLTHERMALENG.2015.12.117>.
- [35] S. Gururatana, S. Skullong, Heat transfer augmentation in a pipe with 3D printed wavy insert, *Oct, Case Stud. Therm. Eng.* 21 (2020), 100698, <https://doi.org/10.1016/J.CSITE.2020.100698>.
- [36] A. Sinha, H. Chattopadhyay, A.K. Iyengar, G. Biswas, Enhancement of heat transfer in a fin-tube heat exchanger using rectangular winglet type vortex generators, *Oct. Int. J. Heat Mass Tran.* 101 (2016) 667–681, <https://doi.org/10.1016/J.IJHEATMASSTRANSFER.2016.05.032>.
- [37] A.J. Modi, M.K. Rathod, Experimental investigation of heat transfer enhancement and pressure drop of fin-and-circular tube heat exchangers with modified rectangular winglet vortex generator, *Jun, Int. J. Heat Mass Tran.* 189 (2022), 122742, <https://doi.org/10.1016/J.IJHEATMASSTRANSFER.2022.122742>.
- [38] Y. Li, Z. Qian, Q. Wang, Numerical investigation of thermohydraulic performance on wake region in finned tube heat exchanger with section-streamlined tube, *May, Case Stud. Therm. Eng.* 33 (2022), 101898, <https://doi.org/10.1016/J.CSITE.2022.101898>.
- [39] K. Boukhadia, H. Ameur, D. Sahel, M. Bozit, Effect of the perforation design on the fluid flow and heat transfer characteristics of a plate fin heat exchanger, *December 2017, Int. J. Therm. Sci.* 126 (2018) 172–180, <https://doi.org/10.1016/j.ijthermalsci.2017.12.025>. Apr..
- [40] C.-H. Huang, L.-W. Liu, Optimal position and perforated radius of punched vortex generators for heat sink, *Apr, Case Stud. Therm. Eng.* 32 (2022), 101916, <https://doi.org/10.1016/J.CSITE.2022.101916>.
- [41] Y. Menni, et al., Effects of two-equation turbulence models on the convective instability in finned channel heat exchangers, *Mar, Case Stud. Therm. Eng.* 31 (2022), 101824, <https://doi.org/10.1016/J.CSITE.2022.101824>.

Layanan Perpustakaan UHAMKA

Perforated concave rectangular winglet pair vortex generators enhance the heat transfer of air flowing through heated tubes ...

 Oktarina Heriyani
 Fakultas Teknologi Industri dan Informatika
 Universitas Muhammadiyah Prof. Dr. Hamka

Document Details

Submission ID

trn:oid:::1:3266371804

Submission Date

Jun 2, 2025, 9:52 AM GMT+7

Download Date

Jun 2, 2025, 10:03 AM GMT+7

File Name

Perforated_concave_rectangular_winglet_pair_vortex_generators_enhance_the_heat_transfer_of_....pdf

File Size

8.5 MB

15 Pages

8,337 Words

39,798 Characters

20% Overall Similarity

The combined total of all matches, including overlapping sources, for each database.





Filtered from the Report

- Bibliography




Exclusions

- 7 Excluded Sources
- 15 Excluded Matches

Match Groups

-  **102** Not Cited or Quoted 14%
Matches with neither in-text citation nor quotation marks
-  **47** Missing Quotations 6%
Matches that are still very similar to source material
-  **0** Missing Citation 0%
Matches that have quotation marks, but no in-text citation
-  **0** Cited and Quoted 0%
Matches with in-text citation present, but no quotation marks

Top Sources

- 14%  Internet sources
- 17%  Publications
- 0%  Submitted works (Student Papers)

Integrity Flags

0 Integrity Flags for Review

No suspicious text manipulations found.

Our system's algorithms look deeply at a document for any inconsistencies that would set it apart from a normal submission. If we notice something strange, we flag it for you to review.

A Flag is not necessarily an indicator of a problem. However, we'd recommend you focus your attention there for further review.

Match Groups

- 102** Not Cited or Quoted 14%
Matches with neither in-text citation nor quotation marks
- 47** Missing Quotations 6%
Matches that are still very similar to source material
- 0** Missing Citation 0%
Matches that have quotation marks, but no in-text citation
- 0** Cited and Quoted 0%
Matches with in-text citation present, but no quotation marks

Top Sources

- 14% Internet sources
- 17% Publications
- 0% Submitted works (Student Papers)

Top Sources

The sources with the highest number of matches within the submission. Overlapping sources will not be displayed.

1	Internet	mdpi-res.com	3%
2	Publication	Yafid Effendi, Amrih Prayogo, Syaiful, M. Djaeni, Eflita Yohana. "Effect of perforat...	2%
3	Internet	mts.intechopen.com	1%
4	Internet	eprints.undip.ac.id	1%
5	Internet	iieta.org	<1%
6	Internet	ejers.org	<1%
7	Publication	Syaiful, Ganesha Rachmandala, Bambang Yunianto, MSK Tony Su, M. Ilham Maul...	<1%
8	Internet	www.ej-eng.org	<1%
9	Internet	link.springer.com	<1%
10	Internet	vdoc.pub	<1%

11	Internet	semarakilmu.com.my	<1%
12	Publication	Man-Wen Tian, Saleh Khorasani, Hazim Moria, Samira Pourhedayat, Hamed Sadig...	<1%
13	Internet	trepo.tuni.fi	<1%
14	Publication	Proceedings of ISES World Congress 2007 (Vol I – Vol V), 2009.	<1%
15	Publication	Syaiful, Nakula Kusuma, Muchammad, Retno Wulandari, Nazarudin Sinaga, Ahm...	<1%
16	Publication	Xingyu Liang, Min Min, Kaikai Bian, Junlin Cheng. "Study on the enhanced heat tr...	<1%
17	Publication	"Recent Advances in Computational and Experimental Mechanics, Vol II", Springe...	<1%
18	Internet	air.unimi.it	<1%
19	Internet	coek.info	<1%
20	Internet	www.tandfonline.com	<1%
21	Publication	Mehmet Dogan, Atila Abir İgci. "An experimental comparison of delta winglet an...	<1%
22	Publication	He, Ya-Ling, Pan Chu, Wen-Quan Tao, Yu-Wen Zhang, and Tao Xie. "Analysis of he...	<1%
23	Publication	Mostafa Kamal Fahad, Nowroze Farhan Ifraj, Sharzil Huda Tahsin, Md. Jahid Hasa...	<1%
24	Publication	S. H. Chan. "Transport Phenomena In Combustion, Volume 1 - Proceedings of the ...	<1%

25	Internet	www.iieta.org	<1%
26	Student papers	University of Pretoria	<1%
27	Publication	Mallikarjuna Veerabhadrapa Bidari, P. B. Nagaraj, Gururaj Lalagi. "Influence of d...	<1%
28	Publication	Syaiful, Tri Wahyuni, Bambang Yunianto, Nazaruddin Sinaga. "Evaluation of Vorte...	<1%
29	Publication	Wei Li, Junye Li, Zhaozan Feng, Kan Zhou, Zan Wu. "Local heat transfer in subcool...	<1%
30	Internet	researchmgt.monash.edu	<1%
31	Publication	Mingjie Li, Jingguo Qu, Jianfei Zhang, Jinjia Wei, Wenquan Tao. "Air side heat tran...	<1%
32	Publication	Selma Akcay. "Numerical analysis of heat transfer improvement for pulsating flo...	<1%
33	Publication	Shiquan Zhu, Longjiang Li, Tian Qi, Wenfeng Hu, Chuanxiao Cheng, Shuang Cao, X...	<1%
34	Publication	Waleed A. Abdelmaksoud, Alaa E. Mahfouz, Essam E. Khalil. "Thermal Performanc...	<1%
35	Internet	server.thermalfluidscentral.com	<1%
36	Publication	Nurjannah Hasbullah, Fatimah Al Zahrah Mohd Saat, Fadhilah Shikh Anuar, Moha...	<1%
37	Internet	ijrar.org	<1%
38	Internet	openaccess.biruni.edu.tr	<1%

39	Internet	www.intechopen.com	<1%
40	Internet	www2.mdpi.com	<1%
41	Publication	KeWei Song, WanLing Hu, Song Liu, LiangBi Wang. "Quantitative relationship bet...	<1%
42	Publication	Muhammad Awais, Arafat A. Bhuiyan. "Enhancement of thermal and hydraulic pe...	<1%
43	Publication	Tatemoto, Y.. "Drying characteristics of porous material immersed in a bed of gla...	<1%
44	Internet	c.coek.info	<1%
45	Internet	dergipark.org.tr	<1%
46	Internet	hdl.handle.net	<1%
47	Internet	lirias.kuleuven.be	<1%
48	Internet	repo.ijert.org	<1%
49	Publication	A. Y. Adam, A. N. Oumer, G. Najafi, M. Ishak, M. Firdaus, T. B. Aklilu. "State of the ...	<1%
50	Publication	Anggara Dwita Burmana, Rondang Tambun, Bode Haryanto, Maya Sarah, Vikram ...	<1%
51	Publication	Jamal-Eddine Salhi, Tarik Zarrouk, Tabish Alam, Md Irfanul Haque Siddiqui, Dan D...	<1%
52	Publication	Syaiful, Arsanti Rakha Siwi, Tony Suryo Utomo, Yurianto, Retno Wulandari. "Num...	<1%

53	Publication	Syaiful, M. Kurnia Lutfi. "Numerical Investigation of Heat Transfer and Fluid Flow ..."	<1%
54	Publication	"Proceedings of the 2nd International Conference on Experimental and Computa..."	<1%
55	Publication	Chao Luo, Shuai Wu, Kewei Song, Liang Hua, Liangbi Wang. "Thermo-hydraulic pe..."	<1%
56	Publication	Petar Georgiev, C. Guedes Soares. "Sustainable Development and Innovations in ..."	<1%
57	Publication	Syaiful, Muhammad Untung Zaenal Priyadi, Bambang Yunianto, Nazaruddin Sina...	<1%



Contents lists available at ScienceDirect

Results in Engineering

journal homepage: www.sciencedirect.com/journal/results-in-engineering



Perforated concave rectangular winglet pair vortex generators enhance the heat transfer of air flowing through heated tubes inside a channel

Oktarina Heriyani^{a,b,*}, Mohammad Djaeni^a, Syaiful^{a,**}, Aldila Kurnia Putri^a

^a Mechanical Engineering Department, Engineering Faculty, University of Diponegoro, Semarang, Indonesia

^b Mechanical Engineering Program, Engineering Faculty, University of Muhammadiyah Prof. DR. HAMKA, Jakarta, Indonesia

ARTICLE INFO

Keywords:

Perforated
Rectangular winglet
Concave
Pressure drop
Vortex generator
Heat transfer
Thermal performance

ABSTRACT

A significant increase in the rate heat transfer in a heat exchanger system is made possible by increasing the convection heat-transfer coefficient using a passive method. The addition of vortex generators (VGs) to the fins and tubes of a heat exchanger is currently the most effective passive method. However, the increase in heat was accompanied by an increase in pressure drop. Therefore, in this study, we installed perforated concave rectangular winglet pair vortex generators (PCRWP VGs) on plates in rectangular ducts to increase the heat transfer through the six heated tubes to the air stream by lowering the enhancement in the pressure drop. We attempted to determine the best cost-benefit ratio (CBR) with a fluid flow velocity difference of 0.4–2 m/s at intervals of 0.2 m/s (Reynolds number (Re) of 2143 to 11,763) in the channel. The PCRWP VGs were composed of in-line and staggered configurations. The results showed a lower CBR (3.56) for the in-line configuration than for the staggered configuration. Moreover, the lowest CBR was accompanied by an increase in thermal performance (TEF) of 1.29.

1. Introduction

The global energy demand is expected to triple over the next few years. According to a statement by the International Energy Agency (IEA), the main driver is the increasing use of air conditioning (AC) machines [1]. Thus, promoting energy efficiency in air conditioners is important and requires maximising their thermal performance, which involves increasing the rate of heat transfer in its main component, i.e., the condenser. A condenser, commonly used in air conditioners, comprises a fin and a tube and functions as a refrigerant cooling medium. However, the high thermal resistance (75%) of the fin air side of the condenser lowers the heat-transfer rate in the heat exchanger [2]. Thus, the thermal resistance must be lowered to enhance the heat transfer rate.

A commonly used active methods to increase the rate of heat transfer involves adding vortex generators (VGs), which, according to the research results obtained by Mugisidi et al., increases the performance of a condenser [3]. The added VGs cause longitudinal vortices (LVs), damage the primary flow, make the second flow as large as the first and increase air mixing in the area [4,5]. The size of the LVs, shape of the flow, and mixing are influenced by the shape, geometry and position of

the VGs added to the fins and tubes of the heat exchanger [6].

Samidifat et al. showed that simple rectangular vortex generators (RVGs) can increase the heat transfer rate by 7%; however, this causes a pressure drop in the heat exchanger system [7]. Meanwhile, modified RVGs with a concave shape on the front and rear surfaces decreased the heat transfer performance of the heat exchanger tube. A better option is to use RVGs with a double convex front surface and a single concave back surface, which can strengthen the primary vortex, increasing the rate of heat transfer from the plate to the fluid, as demonstrated in a study by Kashyap et al. [8]. Further research conducted by Kashyap et al. in the same year concluded that modifying the surface shape of rectangular winglet vortex generators (RWVGs) can create longitudinal eddies that interact with the boundary layer, thereby increasing the rate of convection heat transfer [9]. Based on their research, the increase in the optimal heat transfer rate was 14.4. The optimal heat transfer performance was also obtained from the results of experiments conducted by Adnan et al. on rectangular ducts by adding delta and rectangular winglet VGs [10]. Concave curved delta winglet VGs were compared with convex curved delta winglet VGs by Song et al. to observe changes in the heat transfer rate [11]. The results showed that the concave VGs

* Corresponding author. Mechanical Engineering Department, Engineering Faculty, University of Diponegoro, Semarang, Indonesia.

** Corresponding author.

E-mail addresses: oktarina@uhamka.ac.id (O. Heriyani), syaiful.undip2011@gmail.com (Syaiful).

<https://doi.org/10.1016/j.rineng.2022.100705>

Received 12 July 2022; Received in revised form 23 September 2022; Accepted 14 October 2022

Available online 22 October 2022

2590-1230/© 2022 The Authors. Published by Elsevier B.V. This is an open access article under the CC BY-NC-ND license (<http://creativecommons.org/licenses/by-nc-nd/4.0/>).

improved the heat transfer better than the convex VGs. The differences in the shape of the VGs affects the change in the heat transfer rate and the change in the geometry of the VG, such as a new rib geometry in the cylinder channel [12].

Zeeshan et al. showed that increasing the angle of attack increased the rate of heat transfer (to 37.01–64.54%) if a pair of RWVGs were placed at the back of the tube even though this did not reduce the pressure drop [13]. A decrease in the value of the pressure drop also did not occur significantly, even though there was an increase in heat of 260% in heat, as per the results of the research conducted by Linardo et al. using the batched heat and channelled pipe (BHCP) approach [14]. The increase in heat transfer performance is influenced by the number of RWVG pairs based on the research results of Heriyani et al., where there is an increase in the hydraulic thermal performance evaluation criteria by 15.17% for three pairs of RWVG compared with the baseline [15]. Wang et al. found that the more pairs of VGs placed in the crossflow, the higher the increase in the heat transfer coefficient [16]. Sun et al. further discovered that increasing the number of RWVGs in the heat exchanger tube increased the heat transfer, with a maximum thermal enhancement factor (TEF) of 1.27 [17]. The TEF value of a V-delta winglet VG reached 1.82–3% higher than that of a V-rectangular winglet VG, as revealed by Promvong et al. [18]. These results were obtained with an optimal blockage ratio (BR) of 0.15 and pitch ratio (PR) 1.0. Skullong et al. modified the shapes of RWVGs with optimal BRs and PRs to achieve an optimum heat transfer performance and reduced pressure drop; their shape modification involved perforating RWVGs [19].

The positions of the holes in the RWVGs did not significantly affect the increase in heat transfer; however, they significantly affected the flow resistance of the VGs. The heat-transfer rate increased as the height (vertical position) of the hole increased. Widthwise, although there is an initial increase, the heat transfer rate decreased with increasing lateral distance [20]. An increase in the number of holes in the RWVGs indicates an increase in fluid flow, which forces the fluid to flow behind the RWVGs, thereby increasing heat transfer [4]. The heat transfer rate increased during laminar flow when the Reynolds number (Re) increased and then decreased with an increase in Re during turbulent flow [20]. Positioning the tube in-line with a pair of RWVGs in a common flow-down configuration provides better performance than the common flow-up configuration. However, a staggered tube position is

superior, resulting in a 25.85% higher heat-transfer performance than when a pair of RWVGs is not used [21].

In the existing studies, no detailed analyses of heat transfer were conducted on from the surfaces of several cylinders heated and arranged in-line when using a perforated vortex generator. Therefore, the focus herein is on investigating the advantages of using perforated concave rectangular winglet pair vortex generators (PCRWP VGs) to increase the heat transfer of the airflow through heated tubes arranged in-line in the ducts.

2. Experimental approach

2.1. Experimental setup

This research was conducted experimentally with a test equipment scheme comprising a rectangular channel sized $370 \times 18 \times 8$ cm. The duct was made of 1 cm thick glass, as shown in Fig. 1.

Based on Fig. 1, the rectangular channel is equipped with a blower (50 Hz, Wipro with a rated voltage of 220 V), an inverter (Mitsubishi Electric type FR-D700 with an accuracy of 0.01), straightener, hot wire anemometer (Lutron type AM-4204 with an accuracy of 0.1), wattmeter (Lutron DW-6060 with an accuracy ± 1.0), central processing unit (CPU), micromanometer, thermocouple (K type with a temperature interval of -200 – 1250 °C and an accuracy ± 0.5) where one thermocouple was placed in the air inlet area, six thermocouples on the back surface of the tubes and 15 on the outlet side of the wire, data acquisition (Advantech USB-4718 type with an accuracy of 0.001) and heater regulator. The heater was connected to six tubes with a diameter of 19.05 mm and height of 65.8 mm, with each tube having the same power. Total heating power of 40 W was applied to the six tubes using a regulator. The heating air flowing through the tubes occurs via convection. Thus, the air at the outlet side becomes hotter than that at the inlet side.

A pressure micromanometer (Fluke type 922, with an accuracy of ± 0.05) was used to monitor the flow pressure drop. Two pitot tubes, each set 26 cm ahead of the inlet of the test specimen and 2.5 cm behind it, were connected to a micromanometer to measure the pressure drop. The pressure drop measurements were recorded 30 times for 5 sek on at each speed variation. Furthermore, flow visualisation was performed by

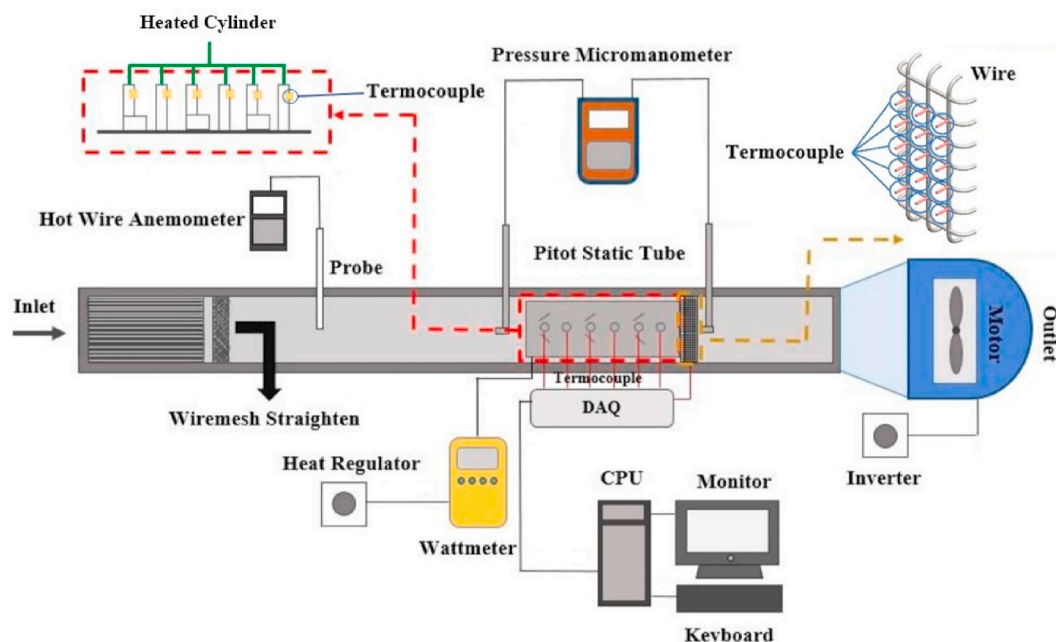


Fig. 1. Experimental tool schematic.

directing the smoke from vaporised fluid in the fluid vaporator into the mainflow.

The VGs used as test specimens were perforated rectangular winglet pair (PRWP) and perforated concave rectangular winglet pair (PCRWP) vortex generators (VGs). Perforated is a term for holes in the VGs, as shown in Fig. 2. The VGs have dimensions of the same length and width of 30 mm, with 36 holes. The bore diameter on the VGs was 2.5 mm. The distance between the holes was 5 mm from the center.

The VGs are placed on an aluminium plate measuring $500 \times 165 \times 1$ mm. The geometry and the pitch between VGs for both in-line and staggered configurations are shown in Fig. 3, with an angle of attack (α) of 150 [2]. The distance between the cylinders is 120 mm, with a cylinder diameter of 19.05 mm.

The VGs configurations were arranged in-line and staggered on the plate. The perforated rectangular winglet (PRW) and perforated concave rectangular winglet (PCRW) VGs in-line configurations with one, two and three pairs are shown in Fig. 4. For each pair, the VGs were placed

on the left and right sides of the first row of tubes. VGs were placed in the first- and third-row tubes for two pairs. For the three pairs, VGs were placed on the first-, third-, and fifth-row tubes.

The PRW and PCRW VGs staggered configurations with one, two, and three pairs are shown in Fig. 5. For one pair, the VGs are placed on the right side of the first-row tube and on the left side of the second. The VGs are placed on the right side of the first and third row tubes and on the left side of the second and fourth tubes for two pairs. For the three pairs, the VGs are placed on the right side of the first, third and fifth rows of the tubes and on the left side of the second, fourth and sixth tubes.

2.2. Parameter definitions

The parameters in this study were derived from the equation used by Oneissi et al. to obtain the thermal enhancement factor (TEF) [22].

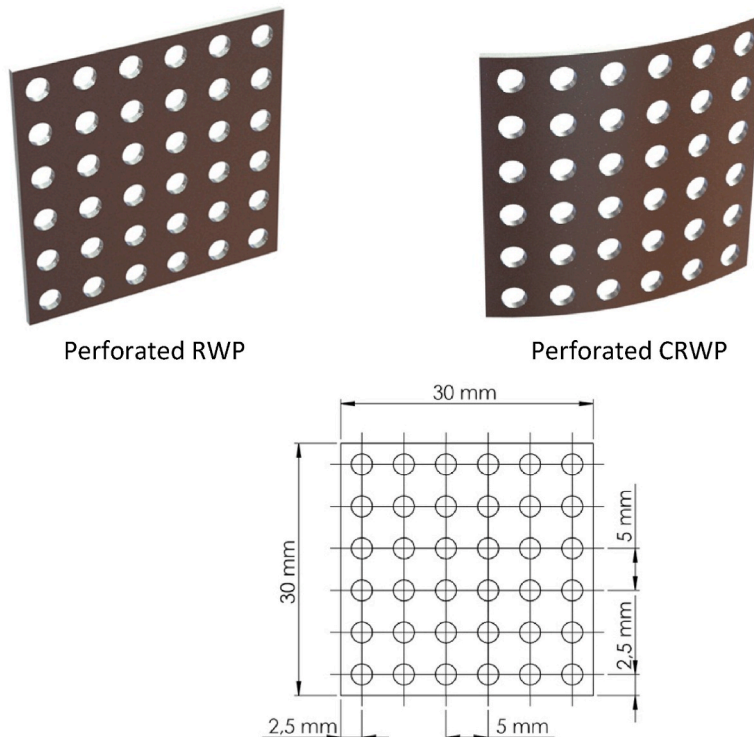


Fig. 2. Geometry of the VGs.

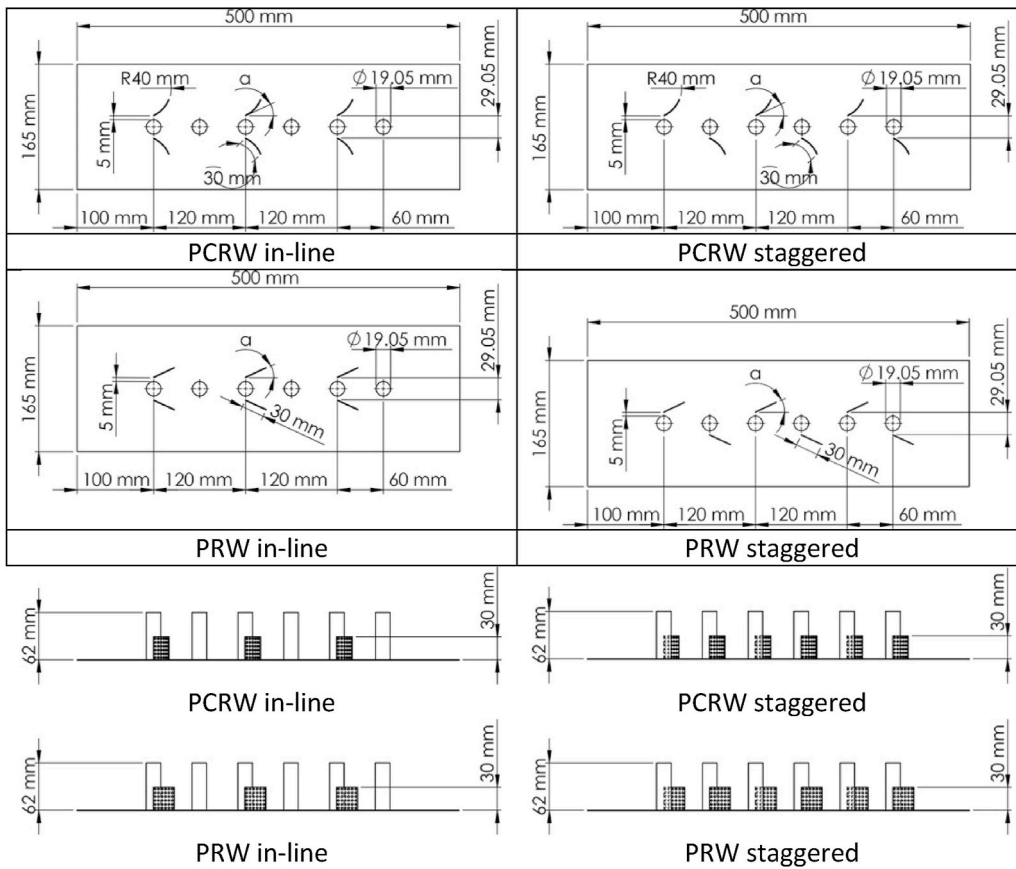


Fig. 3. Geometry and pitch of the VGs.

$$TEF = \frac{Nu}{Nu_0} \left(\frac{f}{f_0} \right)^{\frac{1}{3}} \quad (1)$$

The Nusselt number and friction factor for the baseline conditions are symbolised as (Nu_0) and (f_0) , and (Nu) and (f) based on the research of Zeeshan et al. [23]

$$Nu = \frac{q D_h}{A_{tube} \Delta T_{LMTD} k} \quad (2)$$

$$h = \frac{q}{A_{tube} \Delta T_{LMTD}} \quad (3)$$

$$q = \dot{m} c_p (T_{out} - T_{in}) \quad (4)$$

where D_h , A_{tube} , ΔT_{LMTD} , \dot{m} , c_p , T_{out} and T_{in} , are hydraulic diameter, tube surface area, log mean temperature difference, mass flow rate, specific heat, outlet temperature, and inlet temperature, respectively

$$D_h = \frac{4A_c}{p} = \frac{4ab}{2(a+b)} = \frac{2ab}{a+b} \quad (5)$$

$$\Delta T_{LMTD} = \frac{(\bar{T}_{tube} - \bar{T}_{out}) - (\bar{T}_{tube} - \bar{T}_{in})}{\ln[(\bar{T}_{tube} - \bar{T}_{out}) - (\bar{T}_{tube} - \bar{T}_{in})]} \quad (6)$$

where A_c and T_{tube} are channel surface area and tube temperature, respectively.

The result of D_h is used to calculate Re with the formula

$$Re = \frac{\rho u_{in} D_h}{\mu} \quad (7)$$

and friction factor (f) was determined to evaluate the performance of hydro dynamic using

$$f = \frac{2\Delta P D_h}{\rho V^2 (L + 6D)} \quad (8)$$

where ρ , V , and L are the air density, inlet airflow velocity and length of the test specimen, respectively.

The equation required to determine the cost-benefit ratio (CBR), defined as the ratio of pressure drop per variation in Nu number, as formulated by Tian et al. [25], is as follows:

$$CBR = \frac{\% \Delta P}{\% Nu} \quad (9)$$

This concept investigates whether the method used to enhance the heat-transfer rate is economically efficient. In the hydrodynamic test, the pressure drop (ΔP) is measured by the pressure difference on the sides of P_{inlet} and P_{outlet} of the test specimen in the tested part using equation (10):

$$\Delta P = P_{inlet} - P_{outlet} \quad (10)$$

2.3. Validation

The current study is a follow-up investigation to the work of Yafid et al. [24], and the experimental setup was similar to that of Yafid et al. The difference between the current study and the experiment of Yafid et al. is a test object in which the current study uses concave rectangular winglet (CRW) VGs; in Yafid et al.'s experiment concave delta winglet (CDW) VGs are used. Whitaker et al. [25] studied the heat transfer characteristics of airflow through a single cylinder in a rectangular duct. The results of Yafid et al. were valid, and the same experimental set-up was determined. The Nu value from the experiment of Yafid et al. were comparable with the Nu values from the experiments of Whitaker et al. in the Reynolds number (Re) range of 2143 to 11,763.

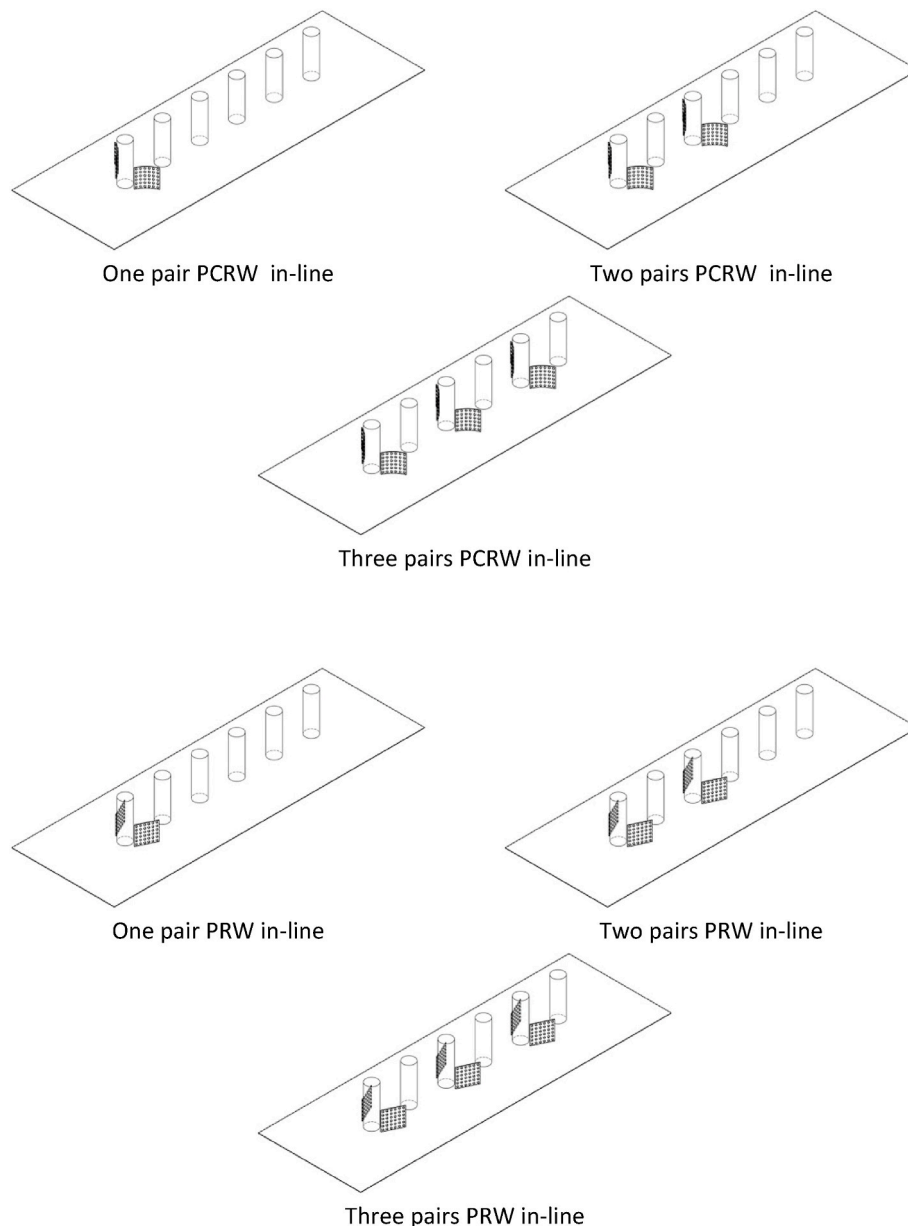


Fig. 4. VGs pairs in-line configurations.

3. Results and discussion

3.1. Flow visualisation

A flow visualisation test was performed to observe the longitudinal vortices (LV) formed after the flow passed through the VGs in the rectangular channel. This test was conducted under low-light conditions to clarify the LV. The laser beam was refracted by a cylindrical glass (diameter 5 mm), which produced a cross-sectional area perpendicular to the direction of the flow. Smoke formed from the evaporation of the liquid was used to visualise the LV in the flow. The VGs used in this visualisation test were PRWP and PCRWP with an in-line arrangement, as shown in Fig. 6.

In Fig. 6 (c) and (d), the PCRWP VGs appear to produce longitudinal vortices (LV) in a wide flow area compared with the PRWP VGs in Fig. 6 (a) and (b) downstream. The back region of the PCRWP VGs had a wider frontal surface area than the PRWP VGs. Consequently, mixing the near-fluid the channel walls with the fluid in the mainstream is better, meaning that the heat transfer rate is increased [26]. Downstream, the

LV compression in the wake area increases the fluid flow velocity passing through the cylindrical structure, thereby increasing the heat transfer rate from the channel surface to the fluid flow in the wake region [27]. The increase in heat transfer produced when using PCRWP VGs was better than that with PRWP VGs.

3.2. Perforated vortex generators effect on heat transfer

The increase in the convection heat transfer was due to the mixing of fluids caused by the strong longitudinal vortices (LVs) [28]. The strength of the LVs is caused by the amount of VGs sets; increasing the amount of VGs pairs in the test specimen can increase the coefficient of the convection heat transfer [29], as shown in Fig. 7.

In Fig. 7, we can see the convective heat transfer coefficient with respect to the Reynolds number (Re), analysed after installing the PCRWP and PRWP with pairs ranging from one, two and three, arranged in-line or staggered. Based on Fig. 7, the convective heat transfer coefficient increased with a rise in Re due to an increase in flow vortices and high turbulence intensity in the channel [30], alongside a reduction in

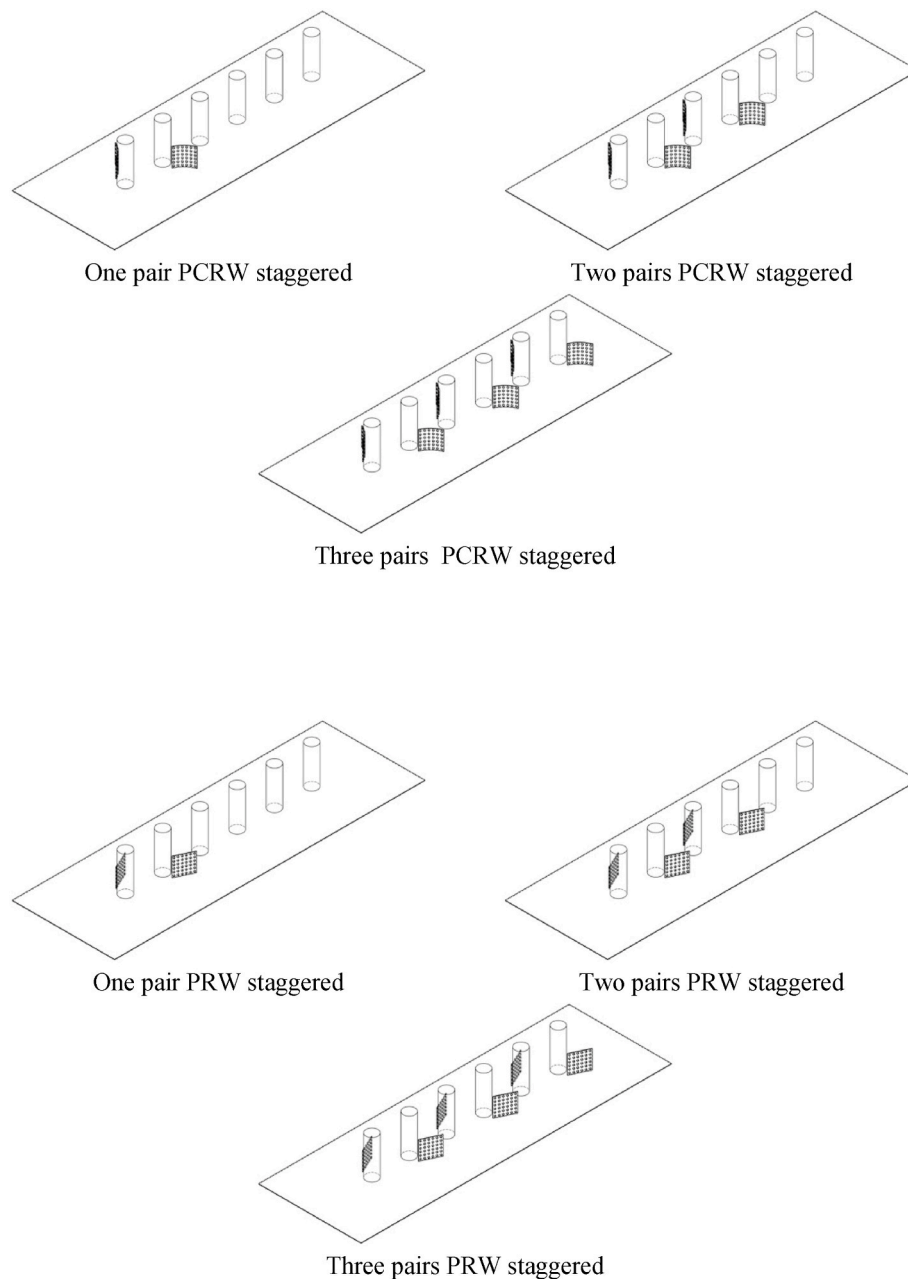


Fig. 5. VGs pairs staggered configurations.

the wake region and stagnation area for each increase in flow velocity [31]. The improve in heat transfer for the staggered was better than that for the PCRW VGs with any number of pairs at the highest Re (11,000). The results in Fig. 7 show that the PCRWP VGs worked better than the PRWP VGs, and the staggered arrangement of the former, with three pairs, gave the highest yield ($153.5 \text{ W/m}^2 \cdot \text{K}$), as shown in Fig. 7(c). Two PCRW pairs ($137.33 \text{ W/m}^2 \cdot \text{K}$, Fig. 7(b)) were better than one ($132.25 \text{ W/m}^2 \cdot \text{K}$) (Fig. 7(a)) because the VGs with a concave surface destabilise the force of centrifugal of the fluid flow, strengthening the flow vortices and making the mixing of the hot fluid near the wall with the cold fluid of the main flow more robust [32]. In Fig. 7(a), the convection heat-transfer coefficient for the case of the in-line PRW VGs has the same value as that of the in-line or staggered PCRW VGs in a pair of VGs. In one pair of VGs, a longitudinal vortex is generated after the flow hits and weakens the VGs [29]. This result contrasts with the cases with two and three pairs of VGs, where the longitudinal vortex produced after striking the first VGs is amplified again when the flow strikes the second

VGs and so on. Therefore, the value of the heat transfer coefficient in the case of a pair of PRW VGs is the same value as that of PCRW VGs at Reynolds numbers above 8000.

3.3. Effect of perforated vortex generators on pressure drop

Using VGs can affect the increase in heat transfer, but there is often an accompanying increase in pressure drop, as shown in Fig. 8, where an increase in pressure drop can be seen along with the increases in Re and pair numbers for both the VG types PCRW and PRW. In general, the highest pressure drop was observed using the PCRWP VGs with a staggered configuration for all Re , except for one pair of VGs. The highest pressure drop was found in the PRWP VGs with an in-line configuration at Re greater than 8000. The pressure drop on the staggered VGs was found to be higher than that on the in-line configuration because of the shorter distance between the VGs of the staggered configuration than that of the in-line [29], caused by the resistance of fluid flow against the

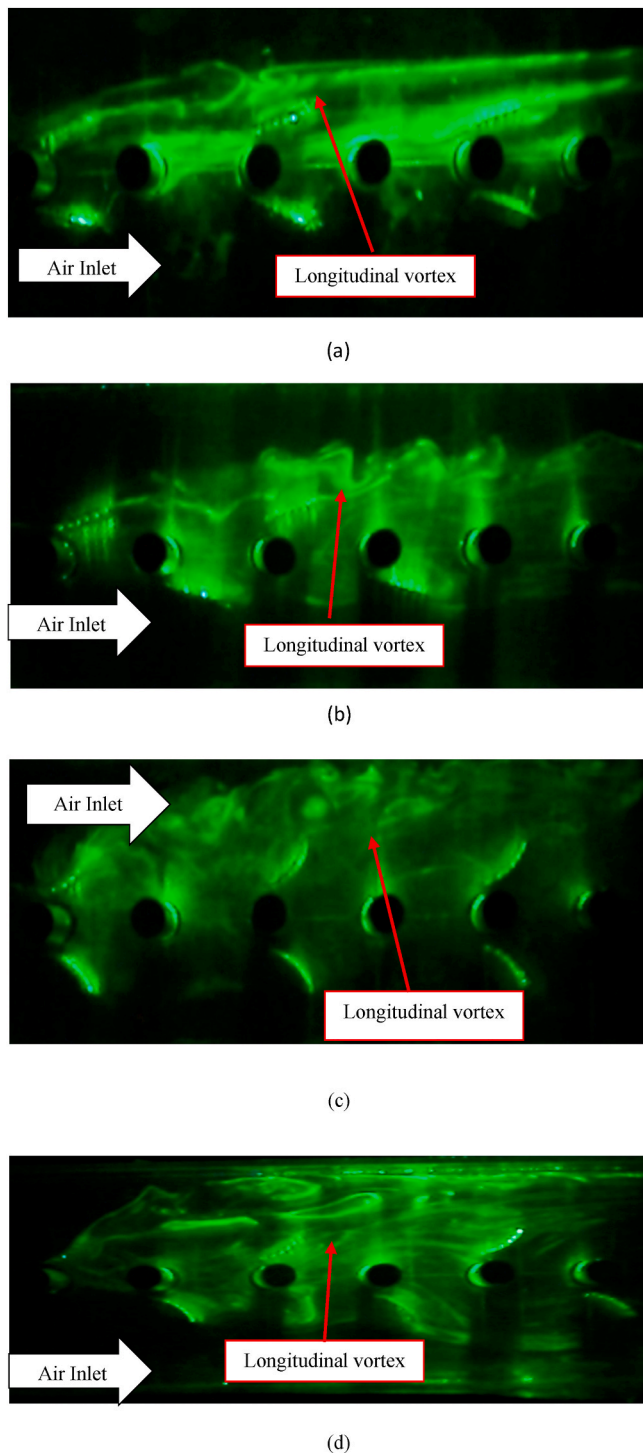


Fig. 6. Visualisation of LV generated by (a) in-line PRWP, (b) staggered PRWP, (c) in-line PCRWP and (d) staggered PCRWP.

walls of the VGs and the expansion of the frontal zone of the VGs in the next-pair arrangement [33]. The pressure drop in the staggered arrangement was lower than that in the in-line arrangement, whereas the PRW VGs type created a lower pressure drop than the PCRW VGs because the latter reduced the frontal area hit by the airflow, resulting in a decrease in drag [34]. In addition, the jet flow from the VG hole can reduce the stagnation flow, which can reduce the pressure drop [35]. A significant decrease in the pressure drop was due to the VG perforation [36]. The best pressure drop value for one pair with a staggered arrangement was 4.58 Pa (see Fig. 4(a)), whereas two pairs (5 Pa, Fig. 4

(b)) were better than three (5.4 Pa, Fig. 4(c)).

3.4. Effect of perforated VGs on thermal enhancement factor

TEF exhibited the hydraulic thermal performance while using VGs, which played a role in restructuring the incoming fluid flow pattern. The increase in the TEF was due to the influence of complex overlapping structures, which meant that the flow developed into a turbulent structure, significantly affecting the heat transfer increase [37]. The experimental TEF values are shown in Fig. 9.

The TEF is the thermal-hydraulic performance which is the ratio of the increase in heat transfer to the pressure drop ratio. In general, the highest TEF was observed when the PCRWP VGs were used with a staggered configuration, as depicted in Fig. 9. The PCRW creates wider flow vortices that can reduce the wake area behind the cylinder. Reducing the wake area can reduce the recirculation zone, affecting the heat transfer from the back of the cylinder to the stream [26]. A large-radius, high-intensity anterior-posterior vortex can reduce the wake area. A lessening within the wake zone increased the flow velocity behind the tube and reduced the recirculation area, resulting in increased heat transfer in this area [27,38]. As shown in Fig. 9, there was an increase in the TEF with greater pairs of VGs used for both the PCRW and PRW VG because the PCRW produced wider flow vortices, which reduced the wake region behind the cylinder, thereby reducing the recirculation zone and impacting the heat transfer increment from the rear cylinder surface to the stream [39]. In this process, a large number of longitudinal vortices with high intensities can reduce the wake area, which increases the flow velocity downstream of the tube and reduces the recirculation region, leading to an increased heat-transfer rate in the region [40,41]. Based on Fig. 9, the best TEF increase occurred at Re between 8000 and 9000. The best TEF values, with one, two and three pairs occurred in the staggered arrangement with PCRW VGs, at 1.18, 1.20 and 1.29, respectively (see Fig. 9).

3.5. Effects of perforated VGs on the cost-benefit ratio

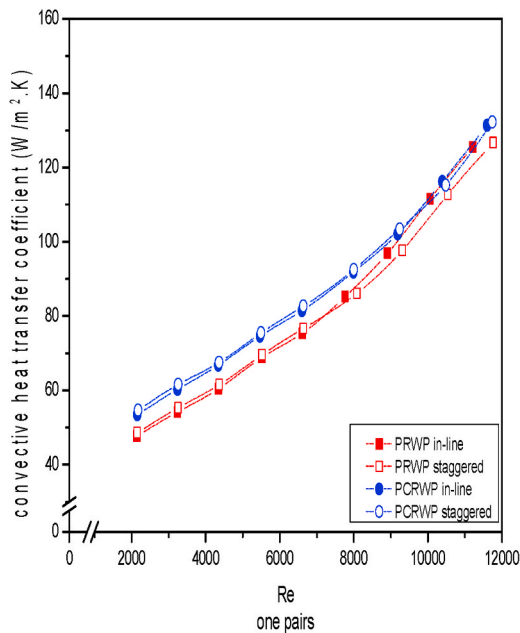
Economic evaluation cannot be conducted based only on the TEF and the net profit from the heat load of the transferred unit [26]. Instead, it must be determined by evaluating the economic value of the heat-transfer improvement by calculating the cost benefit ratio (CBR), as shown in Fig. 10.

Fig. 10 show the result of the CBR calculation to compare the percentage increase in the pressure drop with the percentage increase in the Nusselt number when using VGs. These results indicate that a lower CBR improves thermal performance, which is greater than the drag force [25]. The greatest increase in CBR occurred with the PRW VGs, with an in-line arrangement, totalling 4.57, 4.95 and 3.56 for one, two and three pairs, respectively. The lowest CBR was measured when three sets of PCRW vortex generators with a staggered arrangement were used. The lowest CBR were obtained with the three pairs of staggered-type VGs PCRW. The three VG pairs showed a lower CBR than the one and two pairs because they resulted in the greatest increase in the Nusselt number, accompanied by a lower pressure drop increase, which lowered the CBR. These results show that a lower CBR improves thermal performance relative to resistivity [26]. A low value CBR indicates a more economical value using VGs. In general, using PCRWP VGs with a staggered configuration is the best.

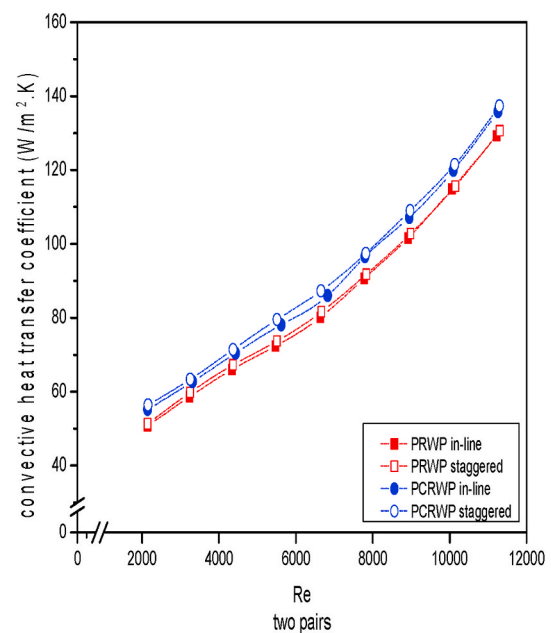
3.6. Heat loss analysis

Heat loss analysis was performed by considering the convection heat transfer from the six tubes to the surrounding fluid flow. The heat transfer rate was calculated for laminar and turbulent flows.

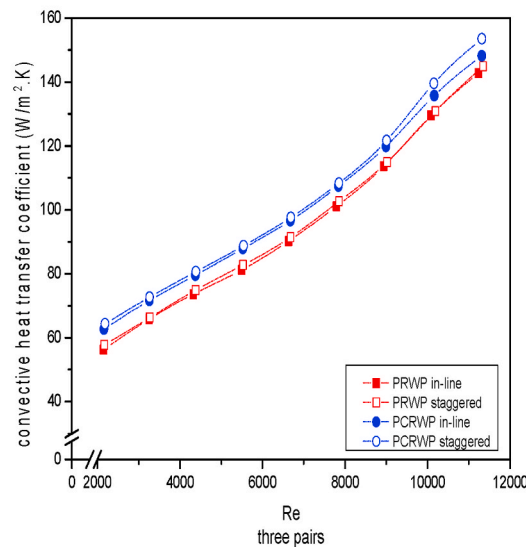
The heat loss in this experiment was calculated by calculating the difference between the induced electric power and total heat through convection from the surface of the tubes to the fluid. In this experiment,



(a)



(b)



(c)

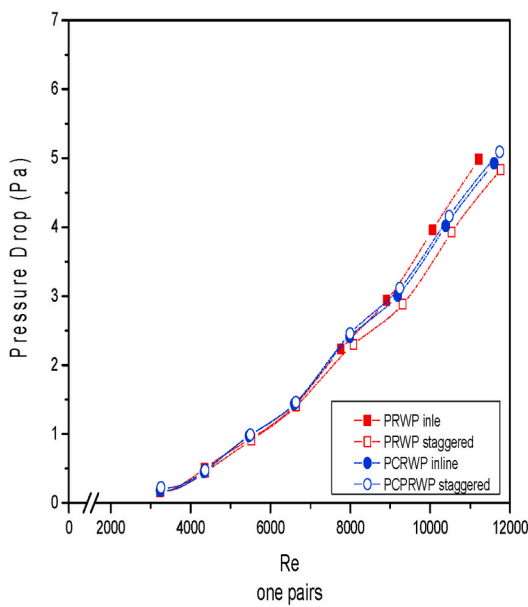
Fig. 7. Graphs of convective heat-transfer coefficient against Reynolds number: (a) one, (b) two and (c) three pairs.

six tubes in a wind tunnel were heated using a heater at a power of 40 W; the velocity of the inlet fluid is varied from 0.4 to 2 m/s at intervals of 0.2 m/s or in the Reynolds number range from 2143 to 11,763. Based on the Reynolds number range, two types of flows were determined; laminar and turbulent. Therefore, the heat loss was determined from the correlation between laminar at 0.4 m/s and turbulent for other velocities. The experimental data for the hydraulic diameter D_h , tube surface area A_{tube} , channel surface area A_c and air specific heat c_p are 0.09223 m, 0.02338908 m², 0.01056 m² and 1.007 J/kgK, respectively. Table 1 is a baseline for calculating heat loss

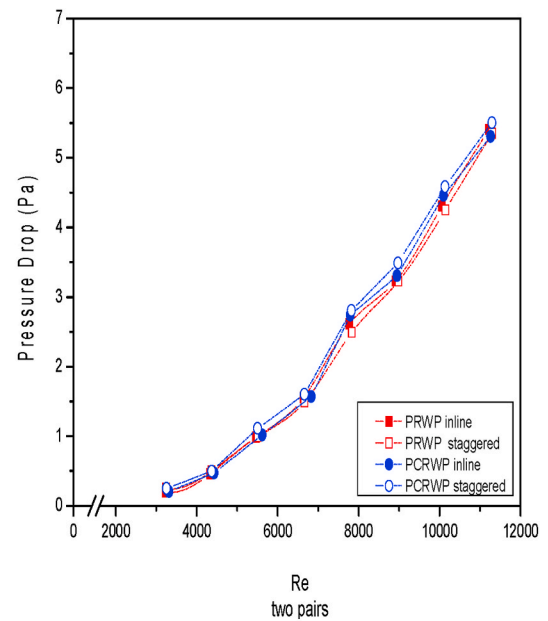
From Table 1, the greater the velocity with an increase in the Re , the lower the heat loss. It can be observed that the heat flow from the heater not only spreads into the tube, but convection also occurs outside the

tube. The heat output increased with Re , i.e., the higher the flow velocity, the greater the turbulence through the cylinder and the higher the turbulence intensity. An increase in the turbulence intensity between a cold airflow and hot cylinder with a constant surface temperature is caused by the airflow velocity [26]. In row-tube arrays, this recirculation area increased for the second and subsequent columns. A lower air velocity in the circulation region indicated less airflow in the region participating in the local heating process [37]. The heat loss under all conditions in this experiment is listed in Table 2.

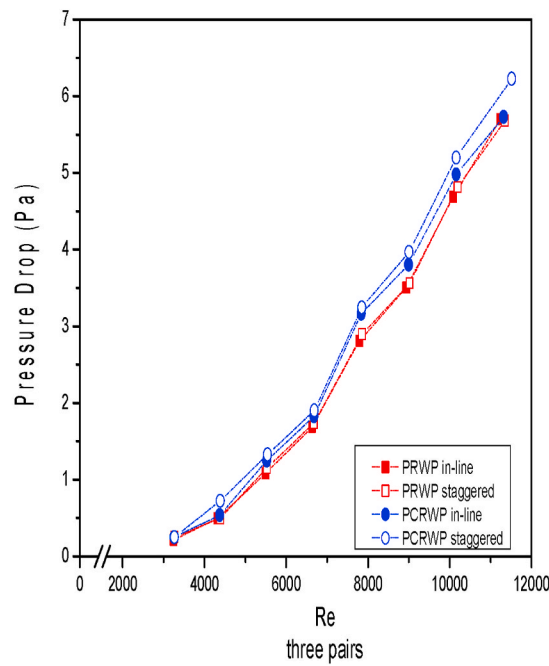
Table 2 shows that the lowest heat loss occurs when three sets of PCRWPs are staggered. The placement of the VGs can increase heat transfer in square ducts as the VGs create longitudinal vortices, which in turn increase vortex strength in the wake region downstream of the tube.



(a)



(b)



(c)

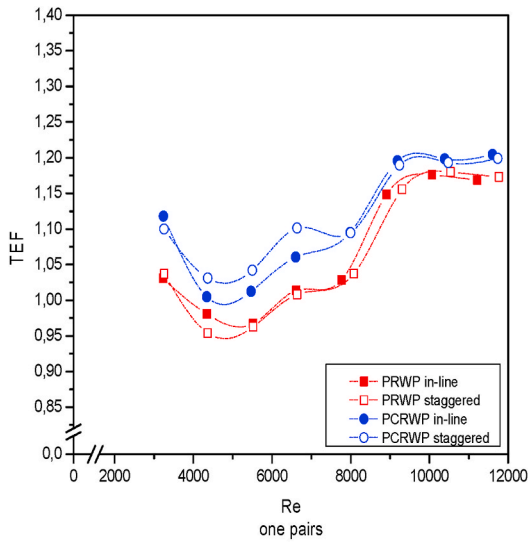
Fig. 8. Graph of pressure drop against Reynolds number: (a) one, (b) two and (c) three pairs.

Longitudinal vortices make the overall temperature field more uniform, improve heat mixing and boundary layer modification, and improve heat transfer performance. A higher number of vortex generators creates more longitudinal vortices and significantly increases heat transfer [26, 29].

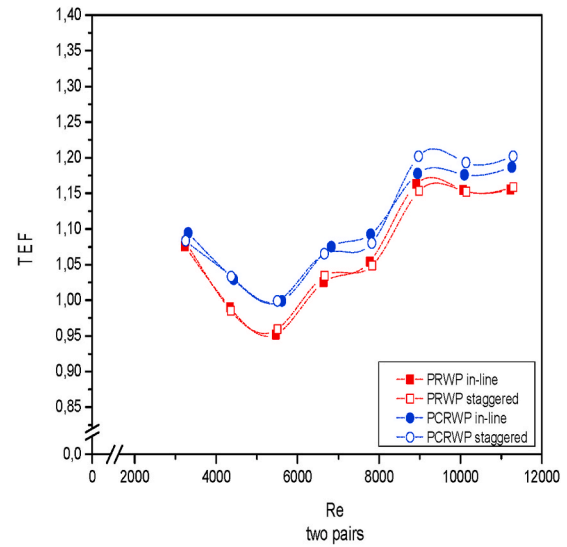
3.7. Uncertainty analysis

In this section, uncertainty analysis calculation data will be shown for the temperature at base-line conditions with a velocity of 0.4 m/s as shown in Table 3.

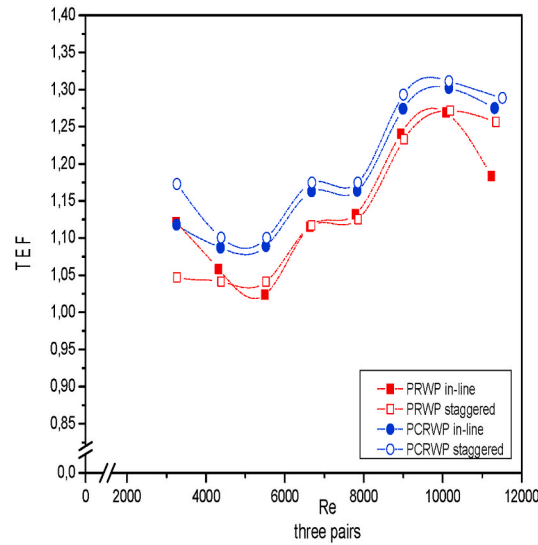
From these data, it is found that \bar{T}_{Tube} can be calculated by the equation as



(a)



(b)



(c)

Fig. 9. Graph of thermal enhancement factor against Reynolds number: (a) one, (b) two and (c) three pairs.

$$\bar{T}_{Tube} = \frac{\bar{T}_{Tube1} + \bar{T}_{Tube2} + \bar{T}_{Tube3} + \bar{T}_{Tube4} + \bar{T}_{Tube5} + \bar{T}_{Tube6}}{6} = 49.56^{\circ}\text{C} \quad (11)$$

Then, the average standard deviation is obtained by the following formula.

$$s_{tube} = \sqrt{\frac{\sum_{i=1}^N (T_{tubei} - \bar{T}_{tube})^2}{N(N-1)}} = 0.029 \quad (12)$$

Therefore, the average T_{tube} can be written as $49.5 \pm 0.029^{\circ}\text{C}$. \bar{T}_{out} calculation results obtained 32.95°C . The average standard deviation was calculated using the following equation:

$$s_{Tout} = \sqrt{\frac{\sum_{i=1}^N (T_{outi} - \bar{T}_{out})^2}{N(N-1)}} = 0.051 \quad (13)$$

Furthermore, the average value of T_{out} can be written as $32.95 \pm$

0.051°C . Using the same equation, the standard deviation of T_{in} was found to be 0.033 . Thus, the average T_{in} value was $29.75 \pm 0.016^{\circ}\text{C}$.

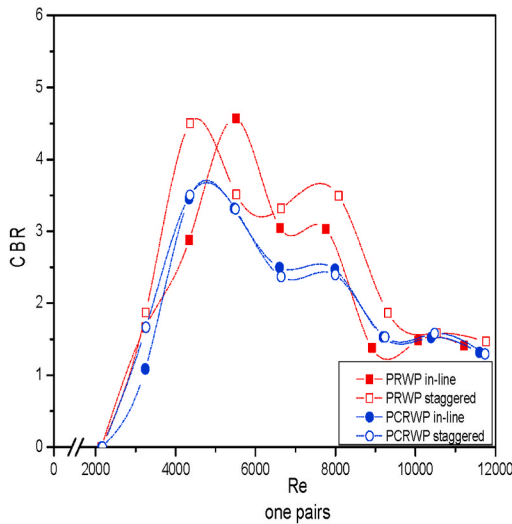
The value of q at a speed of 0.4 m/s was found to be 19.48 W . To determine of the standard deviation of q , the following equation was used:

$$RSS_q = \sqrt{\left(s(\Delta T_{out}) \frac{\partial q}{\partial T_{out}}\right)^2 + \left(s(\Delta T_{in}) \frac{\partial q}{\partial T_{in}}\right)^2} \quad (14)$$

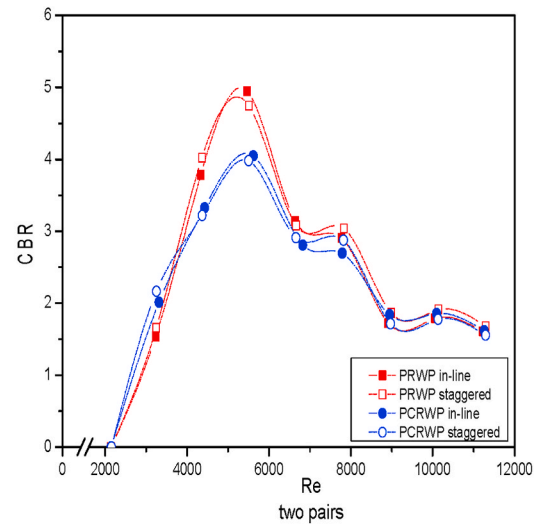
$$\frac{\partial q}{\partial T_{out}} = \frac{\partial(m \cdot c_p \cdot T_{out} - m \cdot c_p \cdot T_{in})}{\partial T_{out}} = m \cdot c \cdot p$$

$$\frac{\partial q}{\partial T_{in}} = \frac{\partial(m \cdot c_p \cdot T_{out} - m \cdot c_p \cdot T_{in})}{\partial T_{in}} = -(m \cdot c \cdot p)$$

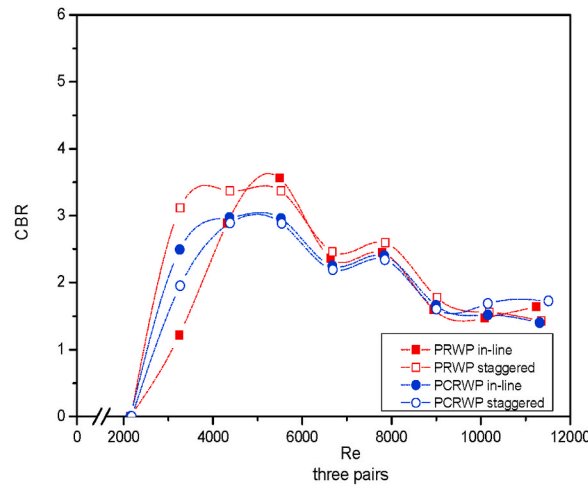
where $s(\Delta T_{out}) = 0.051^{\circ}\text{C}$ and $s(\Delta T_{in}) = 0.033^{\circ}\text{C}$, ensuring, that $RSS_q =$



(a)



(b)



(c)

Fig. 10. Graph of cost-benefit ratio against Reynolds number: (a) one, (b) two and (c) three pairs.

± 0.290 W. Therefore, the heat transfer rate q becomes 19.48 ± 0.290 W. The value of ΔT_{lmd} at a speed of 0.4 m/s was found to be 18.56 °C. To determine the value of the standard deviation of ΔT_{lmd} we used the following equation:

$$\frac{\partial(\Delta T_{lmd})}{\partial T_{out}} = \frac{\partial \left(\frac{(T_{tube} - T_{out}) - (T_{tube} - T_{in})}{\ln \frac{T_{tube} - T_{out}}{T_{tube} - T_{in}}} \right)}{\partial T_{out}}$$

$$RSS_{\Delta T_{lmd}} = \sqrt{\left(s(\Delta T_{tube}) \frac{\partial(\Delta T_{lmd})}{\partial T_{tube}} \right)^2 + \left(s(\Delta T_{out}) \frac{\partial(\Delta T_{lmd})}{\partial T_{out}} \right)^2 + \left(s(\Delta T_{in}) \frac{\partial(\Delta T_{lmd})}{\partial T_{in}} \right)^2} \quad (15)$$

$$\frac{\partial(\Delta T_{lmd})}{\partial T_{tube}} = \frac{\partial \left(\frac{(T_{tube} - T_{out}) - (T_{tube} - T_{in})}{\ln \frac{T_{tube} - T_{out}}{T_{tube} - T_{in}}} \right)}{\partial T_{tube}}$$

$$\frac{\partial(\Delta T_{lmd})}{\partial T_{in}} = \frac{\partial \left(\frac{(T_{tube} - T_{out}) - (T_{tube} - T_{in})}{\ln \frac{T_{tube} - T_{out}}{T_{tube} - T_{in}}} \right)}{\partial T_{in}}$$

Table 1
Heat loss baseline.

	v (m/s)	Re	Mass flow rate (kg/s)	Density (kg/m ³)	Dynamics viscous (kg/ms)	k	Pr	T inlet (C)	T outlet (C)	T tube (C)	ΔT LMTD	ΔT (T tube - T inlet)	Nu	h (W/mK)	q conv (W)	q input (W)	q loss (W)
baseline	0.4	2165	0.004757	1.13	1.9.E-05	0.03	0.73	29	33	50	19	21	155	45	19.48	40	20.52
	0.6	3291	0.00719	1.13	1.9.E-05	0.03	0.73	28	31	46	16	18	174	50	18.98	40	21.02
	0.8	4413	0.009618	1.14	1.9.E-05	0.03	0.73	28	30	44	15	16	192	50	19.19	40	20.81
	1	5545	0.012056	1.14	1.9.E-05	0.03	0.73	28	30	43	14	15	214	55	19.84	40	20.16
	1.2	6661	0.014477	1.14	1.9.E-05	0.03	0.73	28	29	43	14	15	228	61	21.15	40	18.85
	1.4	7826	0.016958	1.15	1.9.E-05	0.03	0.73	28	29	41	12	13	247	70	20.30	40	19.70
	1.6	8965	0.019407	1.15	1.9.E-05	0.03	0.73	27	29	40	12	13	263	75	21.03	40	18.97
	1.8	10,110	0.021863	1.15	1.9.E-05	0.03	0.73	27	28	39	12	12	296	84	22.54	40	17.46
	2	11,272	0.024341	1.15	1.9.E-05	0.03	0.73	27	28	38	11	11	342	97	24.17	40	15.83

Table 2

Calculation of heat loss for the whole case.

type VGs	q conv (W)	q input (W)	q loss (W)
Baseline	20.74	40	19.26
PCRWPI1	25.15	40	14.85
PCRWPI2	27.55	40	12.45
PCRWPI3	27.61	40	12.39
PCRWPS1	26.43	40	13.57
PCRWPS2	26.43	40	13.57
PCRWPS3	27.94	40	12.06
PRWPI1	24.09	40	15.91
PRWPI2	27.25	40	12.75
PRWPI3	28.82	40	11.18
PRWPS1	23.94	40	16.06
PRWPS2	26.37	40	13.63
PRWPS3	28.12	40	11.88

Table 3

Base-line test temperature data at a speed of 0.4 m/s.

T (Tube ₁)	T (Tube ₂)	T (Tube ₃)	T (Tube ₄)	T (Tube ₅)	T (Tube ₆)
49.19093	51.21368	48.32313	49.76915	47.80219	51.27142
49.1834	51.17728	48.3156	49.79053	47.7657	51.2639
49.14545	51.16826	48.30655	49.7526	47.7856	51.25489
49.12105	51.17277	48.28214	49.72821	47.76118	51.2594
49.15297	51.20465	48.28515	49.73122	47.73524	51.2624
49.09966	51.15141	48.28967	49.73573	47.76871	51.26691
49.09815	51.14991	48.23029	49.73423	47.73826	51.29428
49.08912	51.14089	48.25019	49.66739	47.72922	51.22751

where $s(\Delta T_{tube}) = 0,029^\circ C$, $s(\Delta T_{out}) = 0,051^\circ C$ and $s(\Delta T_{in}) = 0,033^\circ C$; we get $RSS_{\Delta T_{lmd}}$ of ± 0.043 , ensuring, that the obtained ΔT_{lmd} is 8.56 ± 0.043 .

The value of Nu at a speed of 0.4 m/s was found to be 155.31. The standard deviation of Nu was obtained using following equation

$$RSS_{Nu} = \sqrt{\left(s(q) \frac{\partial Nu}{\partial Q}\right)^2 + s(\Delta T_{lmd}) \frac{\partial Nu}{\partial \Delta T_{lmd}}} \quad (16)$$

$$\frac{\partial Nu}{\partial q} = \frac{\partial(q \cdot D_h \cdot At^{-1} \cdot \Delta T_{lmd}^{-1} \cdot k^{-1})}{\partial q} = \frac{D_h}{(At)(\Delta T_{lmd})(k)}$$

$$\frac{\partial Nu}{\partial \Delta T_{lmd}} = \frac{\partial(q \cdot D_h \cdot At^{-1} \cdot \Delta T_{lmd}^{-1} \cdot k^{-1})}{\partial \Delta T_{lmd}} = \frac{q \cdot D_h}{(At)(\Delta T_{lmd})^2(k)}$$

With the values of $s(q) = 0.290$ W and $s(\Delta T_{lmd}) = 0.043$, the obtained RSS_{Nu} was ± 2.889 W(m²°C). Therefore, the value of RSS_{Nu} is 155.31 ± 2.889 W/m²°C.

The value of h at a speed of 0.4 m/s was found to be 44.86. To determine the standard deviation of Nu the following equation is used

$$RSS_h = \sqrt{\left(s(Nu) \frac{\partial h}{\partial Nu}\right)^2} \quad (17)$$

$$\frac{\partial h}{\partial Nu} = \frac{\partial(h \cdot D_h \cdot k^{-1})}{\partial h} = \frac{k}{D_h}$$

Furthermore, the value of D_h is 0.092 m and k at $T_f = 40.24$ is 0.026. So the value of h at a speed of 0.4 m/s is:

$$RSS_h = \sqrt{\left(s(Nu) \frac{\partial h}{\partial Nu}\right)^2} = 0,83$$

Thus, the number h at a speed of 0.4 m/s is 44.86 ± 0.83 . So, the error h for the baseline at a speed of 0.4 m/s is

$$Error = \frac{RSS_h}{h} \times 100 \quad (18)$$

Table 4

Baseline pressure drop data at a speed of 2.0 m/s.

ΔP (Pa)			
Data to	2.0 m/s	Data to	2.0 m/s
1	0.013	16	0.012
2	0.013	17	0.013
3	0.013	18	0.012
4	0.013	19	0.012
5	0.012	20	0.013
6	0.013	21	0.013
7	0.013	22	0.012
8	0.012	23	0.013
9	0.013	24	0.012
10	0.013	25	0.013
11	0.013	26	0.013
12	0.013	27	0.013
13	0.012	28	0.013
14	0.012	29	0.012
15	0.013	30	0.012

$$\text{Error} = \frac{0.83}{44.86} \times 100 = 1.51\%$$

From the test in the baseline case with a speed of 2.0 m/s, the results of the pressure drop are listed in Table 4, which show that the average P can be calculated as follows:

$$\overline{\Delta P} = \frac{\Delta P_1 + \Delta P_2 + \Delta P_3 + \dots + \Delta P_{30}}{30} = 3.51 \text{ Pa} \quad (19)$$

The average standard deviation of the pressure drop can then be calculated using the equation

$$s = \sqrt{\frac{\sum_{i=1}^N (\Delta P_i - \overline{\Delta P})^2}{N(N-1)}} = 8.9 \times 10^{-5} \quad (20)$$

Baseline case for the pressure drop value at a speed of 2.0 m/s is $3.51 \pm 8.9 \times 10^{-5}$ Pa. Then, the error in the form of percentage can be calculated using the following equation:

$$\frac{8.9 \times 10^{-5}}{3.51} \times 100 = 0.71$$

The equal calculation approach changed into used for all data. Therefore, the overall error outputs for the pressure-drop vortex generator with placement variations (in-line and staggered), Re and amount of VG sets (one, two and three) are listed in Table 5.

The average TEF results from the experimental results can be calculated as follows.

$$\overline{TEF} = \frac{TEF_1 + TEF_2 + TEF_3 + \dots + TEF_{12}}{12} = 1.12 \quad (21)$$

Then, the average standard deviation of the TEF can be calculated with the equation

Table 5

Overall pressure drop (ΔP).

Vortex Generator Variations	Overall Error P (perforated)
1 PRWP in-line	2.94%
2 PRWP in-line	2.87%
3 PRWP in-line	1.98%
1 PRWP staggered	2.88%
2 PRWP staggered	2.34%
3 PRWP staggered	1.36%
1 PCRWP in-line	2.72%
2 PCRWP in-line	1.80%
3 PCRWP in-line	1.80%
1 PCRWP staggered	2.43%
2 PCRWP staggered	1.91%
3 PCRWP staggered	0.97%

Table 6

Overall error TEF .

Variasi Vortex Generator	Overall Error TEF (Berlubang)
1 RWP in-line	0.47%
2 RWP in-line	0.47%
3 RWP in-line	0.43%
1 RWP staggered	0.47%
2 RWP staggered	0.47%
3 RWP staggered	0.43%
1 CRWP in-line	0.45%
2 CRWP in-line	0.45%
3 CRWP in-line	0.42%
1 CRWP staggered	0.45%
2 CRWP staggered	0.45%
3 CRWP staggered	0.41%

$$s = \sqrt{\frac{\sum_{i=1}^N (TEF_i - \overline{TEF})^2}{N(N-1)}} = 1.07 \quad (22)$$

Therefore, the TEF value was 1.12 ± 1.07 . Then, the error in the form of percentage can be calculated using the following equation:

$$\frac{1.07}{1.12} \times 100 = 0.94\%$$

The overall error results for the TEF vortex generator with placement variations (in-line and staggered), Re and amount of VG sets (one, two and three) are listed in Table 6.

First, find the average CBR of the experimental results with the following formula.

$$\overline{CBR} = \frac{CBR_1 + CBR_2 + CBR_3 + \dots + CBR_{12}}{12} = 2.14 \quad (23)$$

The average standard deviation of the pressure drop CBR can then be calculated using the following equation:

$$s = \sqrt{\frac{\sum_{i=1}^N (CBR_i - \overline{CBR})^2}{N(N-1)}} = 1.60 \quad (24)$$

The CBR value is 2.14 ± 1.60 . Then the error in the form of percentage can be calculated using the following equation:

$$\frac{1.60}{2.14} \times 100 = 0.63\%$$

The overall error results for the CBR vortex generator with placement variations (in-line and staggered), Re and amount of VG sets (one, two and three) are listed in Table 7.

4. Conclusion

Based on the experimental results for perforated concave rectangular winglet pair vortex generators (PCRWP VGs) used to increase the heat transfer of airflow through heated tubes arranged in-line in the duct, we

Table 7

Overall error CBR .

Variasi Vortex Generator	Overall Error CBR (Berlubang)
1 RWP in-line	0.32%
2 RWP in-line	0.29%
3 RWP in-line	0.45%
1 RWP staggered	0.32%
2 RWP staggered	0.31%
3 RWP staggered	0.45%
1 CRWP in-line	0.4%
2 CRWP in-line	0.42%
3 CRWP in-line	0.56%
1 CRWP staggered	0.43%
2 CRWP staggered	0.42%
3 CRWP staggered	0.66%

conclude that using PCRWP VGs affects the convection heat transfer coefficient, pressure drop in achieving hydraulic thermal performance and cost-benefit ratio. In our investigation, the best heat-transfer convection coefficient was $153.5 \text{ W/m}^2 \cdot \text{K}$ for the three pairs of PCRW VGs, in a staggered manner. The greatest improvement in the pressure drop value (4.58 Pa), occurred for one pair of PCRW VGs arranged in a staggered manner, whereas the hydraulic thermal performance was the best (1.29) in this experiment with the three pairs of PCRW VGs arranged in a staggered manner. Finally, the best CBR (3.56) was recorded for the three pairs of PCRW VGs composed in a staggered manner.

Credit author statement

Oktarina Heriyani: Conceptualization, Methodology, Investigation, Writing – original draft preparation.; Mohammad Djaeni: Supervision – Reviewing and Editing.; Syaiful: Conceptualization, Writing – Reviewing and Editing, Conceptualization.; Aldila Kurnia Putri: Visualisation, Validation.

Declaration of competing interest

The authors declare that they have no known competing financial interests or personal relationships that could have appeared to influence the work reported in this paper.

Acknowledgements

The authors would like to thank LEMLITBANG UHAMKA which has funded this research through internal grants from UHAMKA and UPPI UHAMKA what have contributed in facilitating translation and proof reading. The authors also thank the UNDIP thermofluidics laboratory, where the authors carried out this experiment.

References

- [1] R. Sebayang, AC Akan jadi pengkonsumsi listrik utama di Dunia, CNBC Indonesia (2018).
- [2] Z. Qian, Q. Wang, J. Cheng, Analysis of heat and resistance performance of plate fin-and-tube heat exchanger with rectangle-winglet vortex generator, *Int. J. Heat Mass Tran.* 124 (2018) 1198–1211, <https://doi.org/10.1016/j.ijheatmasstransfer.2018.04.037>.
- [3] D. Mugisidi, O. Heriyani, P.H. Gunawan, D. Apriani, Performance improvement of a forced draught cooling tower using a vortex generator, *CFD Lett.* 13 (1) (2021) 45–57, <https://doi.org/10.37934/cfdl.13.1.4557>.
- [4] A.J. Modi, N.A. Kalel, M.K. Rathod, Thermal performance augmentation of fin-and-tube heat exchanger using rectangular winglet vortex generators having circular punched holes, *Int. J. Heat Mass Tran.* 158 (2020) 1–16, <https://doi.org/10.1016/j.ijheatmasstransfer.2020.119724>.
- [5] K.W. Song, T. Tagawa, The optimal arrangement of vortex generators for best heat transfer enhancement in flat-tube-fin heat exchanger, *Int. J. Therm. Sci.* (2018), <https://doi.org/10.1016/j.jthermalsci.2018.06.011>.
- [6] C. Yu, H. Zhang, M. Zeng, R. Wang, B. Gao, Numerical study on turbulent heat transfer performance of a new compound parallel flow shell and tube heat exchanger with longitudinal vortex generator, *May 2019, Appl. Therm. Eng.* 164 (2020), 114449, <https://doi.org/10.1016/j.applthermaleng.2019.114449>.
- [7] M. Samadifar, D. Toghraie, Numerical simulation of heat transfer enhancement in a plate-fin heat exchanger using a new type of vortex generators, *September 2017, Appl. Therm. Eng.* 133 (2018) 671–681, <https://doi.org/10.1016/j.applthermaleng.2018.01.062>.
- [8] U. Kashyap, K. Das, B.K. Debnath, Effect of surface modification of a rectangular vortex generator on heat transfer rate from a surface to fluid, *August 2017, Int. J. Therm. Sci.* 127 (2018) 61–78, <https://doi.org/10.1016/j.jthermalsci.2018.01.004>.
- [9] U. Kashyap, K. Das, B.K. Debnath, Effect of surface modification of a rectangular vortex generator on heat transfer rate from a surface to fluid: an extended study, *August, Int. J. Therm. Sci.* 134 (2018) 269–281, <https://doi.org/10.1016/j.jthermalsci.2018.08.020>.
- [10] A.Q. Ibrahim, R.S. Alturahi, Experimental work for single-phase and two-phase flow in duct banks with vortex generators, *Sep, Results in Engineering* (2022), 100497, <https://doi.org/10.1016/j.rineng.2022.100497>.
- [11] K.W. Song, T. Tagawa, Z.H. Chen, Q. Zhang, Heat transfer characteristics of concave and convex curved vortex generators in the channel of plate heat exchanger under laminar flow, *November 2018, Int. J. Therm. Sci.* 137 (2019) 215–228, <https://doi.org/10.1016/j.jthermalsci.2018.11.002>.

- [12] K.A. Hammoodi, H.A. Hasan, M.H. Abed, A. Basem, A.M. Al-Tajer, Control of heat transfer in circular channels using oblique triangular ribs, *Sep, Results in Engineering* 15 (2022), 100471, <https://doi.org/10.1016/j.rineng.2022.100471>.
- [13] M. Zeeshan, S. Nath, D. Bhanja, A. Das, Numerical investigation for the optimal placements of rectangular vortex generators for improved thermal performance of fin-and-tube heat exchangers, *Appl. Therm. Eng.* (2018), <https://doi.org/10.1016/j.applthermaleng.2018.03.006>.
- [14] H. Linardos, G. Mavrogenis, D. Margaritis, Novel designs of LVGs conformations and introduction of Batch Heated and Channeled Pipe for increasing heat transfer efficiency in pipes, *Mar, Results in Engineering* 13 (2022), 100357, <https://doi.org/10.1016/j.rineng.2022.100357>.
- [15] O. Heriyani, M. Djaeni, Syaiful, Thermal-hydraulic performance analysis by means of rectangular winglet vortex generators in a channel: an experimental study, *European Journal of Engineering and Technology Research* 6 (3) (2021) 150–153, <https://doi.org/10.24018/ejers.2021.6.3.2424>.
- [16] C. Wang, Z. Wang, L. Wang, L. Luo, B. Sundén, Experimental study of fluid flow and heat transfer of jet impingement in cross-flow with a vortex generator pair, *Int. J. Heat Mass Tran.* 135 (2019) 935–949, <https://doi.org/10.1016/j.ijheatmasstransfer.2019.02.024>.
- [17] Z. Sun, K. Zhang, W. Li, Q. Chen, N. Zheng, Investigations of the turbulent thermal-hydraulic performance in circular heat exchanger tubes with multiple rectangular winglet vortex generators, *Mar, Appl. Therm. Eng.* 168 (2020), 114838, <https://doi.org/10.1016/j.applthermaleng.2019.114838>.
- [18] P. Promvongse, S. Skullong, Thermo-hydraulic performance in heat exchanger tube with V-shaped winglet vortex generator, *Appl. Therm. Eng.* (2020), <https://doi.org/10.1016/j.applthermaleng.2019.114424>.
- [19] S. Skullong, P. Promthaisong, P. Promvongse, C. Thianpong, M. Pimsarn, Thermal performance in solar air heater with perforated-winglet-type vortex generator, *June, Sol. Energy* 170 (2018) 1101–1117, <https://doi.org/10.1016/j.solener.2018.05.093>.
- [20] Z. Han, Z. Xu, J. Wang, Numerical simulation on heat transfer characteristics of rectangular vortex generators with a hole, *Int. J. Heat Mass Tran.* 126 (2018) 993–1001, <https://doi.org/10.1016/j.ijheatmasstransfer.2018.06.081>.
- [21] C. Luo, S. Wu, K. Song, L. Hua, L. Wang, Thermo-hydraulic performance optimization of wavy fin heat exchanger by combining delta winglet vortex generators, *Appl. Therm. Eng.* (2019), <https://doi.org/10.1016/j.applthermaleng.2019.114343>.
- [22] H. Naik, S. Tiwari, Effect of winglet location on performance of fin-tube heat exchangers with inline tube arrangement, *Int. J. Heat Mass Tran.* 125 (2018) 248–261, <https://doi.org/10.1016/j.ijheatmasstransfer.2018.04.071>.
- [23] M. Zeeshan, S. Nath, D. Bhanja, A. Das, Numerical investigation for the optimal placements of rectangular vortex generators for improved thermal performance of fin-and-tube heat exchangers, *May, Appl. Therm. Eng.* 136 (2018) 589–601, <https://doi.org/10.1016/j.applthermaleng.2018.03.006>.
- [24] Y. Effendi, A. Prayogo, Syaiful, M. Djaeni, E. Yohana, Effect of perforated concave delta winglet vortex generators on heat transfer and flow resistance through the heated tubes in the channel, *Exp. Heat Tran.* 35 (5) (2022) 553–576, <https://doi.org/10.1080/08916152.2021.1919245>.
- [25] S. Whitaker, Forced Convection Heat Transfer Correlations for Flow In Pipes, Past Flat Plates, Single e Cylinders, Single Spheres, and for Flow In Packed Beds and Tube Bundles, Reprinted from, *AIChE J.* (1972).
- [26] M. Awais, A.A. Bhuiyan, Enhancement of thermal and hydraulic performance of compact finned-tube heat exchanger using vortex generators (VGs): a parametric study, *Jun, Int. J. Therm. Sci.* 140 (2019) 154–166, <https://doi.org/10.1016/j.jthermalsci.2019.02.041>.
- [27] A. Gupta, A. Roy, S. Gupta, M. Gupta, Numerical investigation towards implementation of punched winglet as vortex generator for performance improvement of a fin-and-tube heat exchanger, *Mar, Int. J. Heat Mass Tran.* 149 (2020), 119171, <https://doi.org/10.1016/j.ijheatmasstransfer.2019.119171>.
- [28] M.W. Tian, S. Khorasani, H. Moria, S. Pourhedayat, H.S. Dizaji, Profit and efficiency boost of triangular vortex-generators by novel techniques, *Int. J. Heat Mass Tran.* 156 (2020), 119842, <https://doi.org/10.1016/j.ijheatmasstransfer.2020.119842>.
- [29] Y.L. He, P. Chu, W.Q. Tao, Y.W. Zhang, T. Xie, Analysis of heat transfer and pressure drop for fin-and-tube heat exchangers with rectangular winglet-type vortex generators, *Nov, Appl. Therm. Eng.* 61 (2) (2013) 770–783, <https://doi.org/10.1016/j.applthermaleng.2012.02.040>.
- [30] M. Pranita Hendraswari, M.S. Tony, M.F. Soetanto, Heat Transfer Enhancement inside Rectangular Channel by Means of Vortex Generated by Perforated Concave Rectangular Winglets, 2021, <https://doi.org/10.3390/fluids6010043>.
- [31] A. R. Siwi Syaiful, T.S. Utomo, Y. Yurianto, R. Wulandari, Numerical analysis of heat and fluid flow characteristics of airflow inside rectangular channel with presence of perforated concave delta winglet vortex generators, *International Journal of Heat and Technology* 37 (4) (2019) 1059–1070, <https://doi.org/10.18280/IJHT.370415>.
- [32] A. Sinha, H. Chattopadhyay, A.K. Iyengar, G. Biswas, Enhancement of heat transfer in a fin-tube heat exchanger using rectangular winglet type vortex generators, *Oct. Int. J. Heat Mass Tran.* 101 (2016) 667–681, <https://doi.org/10.1016/j.ijheatmasstransfer.2016.05.032>.
- [33] H. Ke, et al., Thermal-hydraulic performance and optimization of attack angle of delta winglets in plain and wavy finned-tube heat exchangers, *Mar, Appl. Therm. Eng.* 150 (2019) 1054–1065, <https://doi.org/10.1016/j.applthermaleng.2019.01.083>.

- [34] A. Arora, P.M.V. Subbarao, R.S. Agarwal, Development of parametric space for the vortex generator location for improving thermal compactness of an existing inline fin and tube heat exchanger, *Apr. Appl. Therm. Eng.* 98 (2016) 727–742, <https://doi.org/10.1016/J.APPLTHERMALENG.2015.12.117>.
- [35] S. Gururatana, S. Skullong, Heat transfer augmentation in a pipe with 3D printed wavy insert, *Oct, Case Stud. Therm. Eng.* 21 (2020), 100698, <https://doi.org/10.1016/J.CSITE.2020.100698>.
- [36] A. Sinha, H. Chattopadhyay, A.K. Iyengar, G. Biswas, Enhancement of heat transfer in a fin-tube heat exchanger using rectangular winglet type vortex generators, *Oct. Int. J. Heat Mass Tran.* 101 (2016) 667–681, <https://doi.org/10.1016/J.IJHEATMASSTRANSFER.2016.05.032>.
- [37] A.J. Modi, M.K. Rathod, Experimental investigation of heat transfer enhancement and pressure drop of fin-and-circular tube heat exchangers with modified rectangular winglet vortex generator, *Jun, Int. J. Heat Mass Tran.* 189 (2022), 122742, <https://doi.org/10.1016/J.IJHEATMASSTRANSFER.2022.122742>.
- [38] Y. Li, Z. Qian, Q. Wang, Numerical investigation of thermohydraulic performance on wake region in finned tube heat exchanger with section-streamlined tube, *May, Case Stud. Therm. Eng.* 33 (2022), 101898, <https://doi.org/10.1016/J.CSITE.2022.101898>.
- [39] K. Boukhadia, H. Ameur, D. Sahel, M. Bozit, Effect of the perforation design on the fluid flow and heat transfer characteristics of a plate fin heat exchanger, *December 2017, Int. J. Therm. Sci.* 126 (2018) 172–180, <https://doi.org/10.1016/j.ijthermalsci.2017.12.025>. Apr..
- [40] C.-H. Huang, L.-W. Liu, Optimal position and perforated radius of punched vortex generators for heat sink, *Apr, Case Stud. Therm. Eng.* 32 (2022), 101916, <https://doi.org/10.1016/J.CSITE.2022.101916>.
- [41] Y. Menni, et al., Effects of two-equation turbulence models on the convective instability in finned channel heat exchangers, *Mar, Case Stud. Therm. Eng.* 31 (2022), 101824, <https://doi.org/10.1016/J.CSITE.2022.101824>.